



# Design of untethered soft material micromachine for life-like locomotion

Xiao-Qiao Wang<sup>1</sup>, Ghim Wei Ho<sup>2,\*</sup>

<sup>1</sup> Department of Electrical and Computer Engineering, National University of Singapore, 4 Engineering Drive 3, Singapore 117583, Singapore

<sup>2</sup> Materials Science & Engineering, National University of Singapore, 9 Engineering Drive 1, Singapore 117575, Singapore

Living organisms composed of composite materials with complex structures support autonomous and intelligent behaviors, such as motility, perception and response to changes of the environment. By studying the biological structures and their environmental interactions, researchers are now using these natural systems as models for building soft material machines. In this review, we discuss materials and machine engineering principles to achieve life-like locomotion and functionalities in untethered soft micromachines. Through the various mechanochemical or physical mechanisms, we show how molecular motion can be collectively amplified into versatile macroscopic deformation by materials engineering across multiple length scales. In controlled ways, mobile micromachines are made to crawl, roll or jump and adaptive to various terrains, typically inspired by the terrestrial animals while propulsion of swimming micromachines are guided by aquatic organisms. Besides, out-of-equilibrium behaviors of living systems, such as cell cycling, have stimulated the design of autonomous movement. Furthermore, we review the recent efforts on robotic locomotion intelligence to achieve adaptive, functional locomotion and navigation in complex environment. We finally provide a critical perspective for the field of soft micromachines, and highlight the key challenges of different material systems that need to be overcome to realize practical use.

**Keywords:** Untethered soft micromachine; Machine engineering; Biomimetic locomotion; Self-propelling; Shape morphing; Somatosensory

## Introduction

Robots now have important roles in various industries, and the robotic technology is expected to be the key frontier to developing autonomous things in the coming decades [1]. Up to date, the majority of robots are made of electrically powered rigid components with pre-programmed tasks, making them incompetent for autonomous navigation and operation in uncertain complex environment. The bulky computing, powering and driving systems also restrict the body size miniaturization and shape compliance, which are highly required for movements and task executions in small confined spaces. Soft robots, on the other

hand, made out of compliant materials and/or flexible structures [2], provide vast opportunities to address these challenges. In contrast to hard-bodied counterparts, the soft or flexible nature allows continuum body deformation and versatile reversible shape transformation, rendering adaptive body shapes and agile movements in complex environment [3–5], and safe interaction with living organisms or fragile objects [6–9]. Besides, the actuation of soft robots can be driven by various external energy sources, therefore exonerating the robot from conventional rigid electrical motors, and enabling an untethered operation and a fully soft body conformation. In the past decade, huge efforts have been dedicated to developing soft robotic materials and structures, including soft actuators [10–16] and flexible/soft sensors [17–23], providing the basis of soft robots progression. Lev-

\* Corresponding author.

E-mail address: Ho, G.W. (elehgw@nus.edu.sg)

eraging on the stimulus responsiveness of functional polymers, soft actuation can be activated by versatile light [24–26], heat [27,28], electrical [4,29], magnetic fields [30–32], pressure [33,34] and chemical reaction stimuli [18,35]. And the flexible sensor systems promise to perform a multitude of sensing functionalities to identify diverse physical or chemical signals from the surrounding environment or produced by the robot itself. Despite achieving good advancements, the contemporary challenge is to build up actuators, sensors and controllers all in one body to create autonomous and functional machines that can move, sense and respond like natural systems. Such high-level embodiments call for new design principles and materials, which are typically inspired by biology.

The intelligence and autonomy of living organisms are supported by natural composites of polymers and minerals with complex hierarchical structures [36,37]. To mimic the biological behaviors, soft matter, that was once used to create passive, single-use materials, is now, in contrast, involved in the design of actively responsive and multifunctional systems, i.e. soft material machines. Though present soft material machines cannot rival the biological models, they are able to mimic some characteristic behaviors of living matters, including agile motility, active sensing and soft manipulation of objects [38]. Upgrading the active soft matters into robotic machines demands rational construction principles and material stratagem, as well as advanced algorithms for machine engineering technologies. In this review, the realizations of life-like locomotion and intelligence in soft material micromachines, benefited from high-performance engineered materials and biological construction principles are showcased. Fig. 1 presents the general roadmap toward the design of untethered soft micromachines with life-like locomotion. Here, we have set limits to the scope of this review in several ways. Our first design consideration is the method of energy input which drives the molecular motion in the active material components to shape change the soft machines. We will focus on light, heat, humidity, solvent and magnetic fields power sources, which allow untethered operations. Optical and magnetic fields powered actuation are currently the most widely used methods in micromachines, offering remote, dexterous and precise control [31]. While light, heat, humidity and volatile solvents triggered actuation are especially important for design of responsive robots delivering autonomous tasks at ambient environment. As for the materials, we will focus on the synthetic and intrinsically soft or flexible matters with Young's moduli in the range of  $10\text{--}10^9$  Pa [10], while excluding biohybrid tissues and rigid material systems. Also, we will constrain the review to microrobots, as defined by robotists, those that scale from a few centimeters down to micrometer range [24], hence we omit the molecular or colloidal particle nanomotors. In addition, we elaborate the biomimetic life-like locomotion types, which mostly rely on reversible and repetitive deformation of body parts to enable effective propulsion. On the basis of various mechanochemical and/or physical mechanisms, we discuss how molecular-level motion in different responsive soft systems can be triggered by light, heat, magnetic fields or humidity stimulus, and amplified into macroscopic deformation by materials engineering across multiple length scales. And we account deformation of soft material micromachines analogous

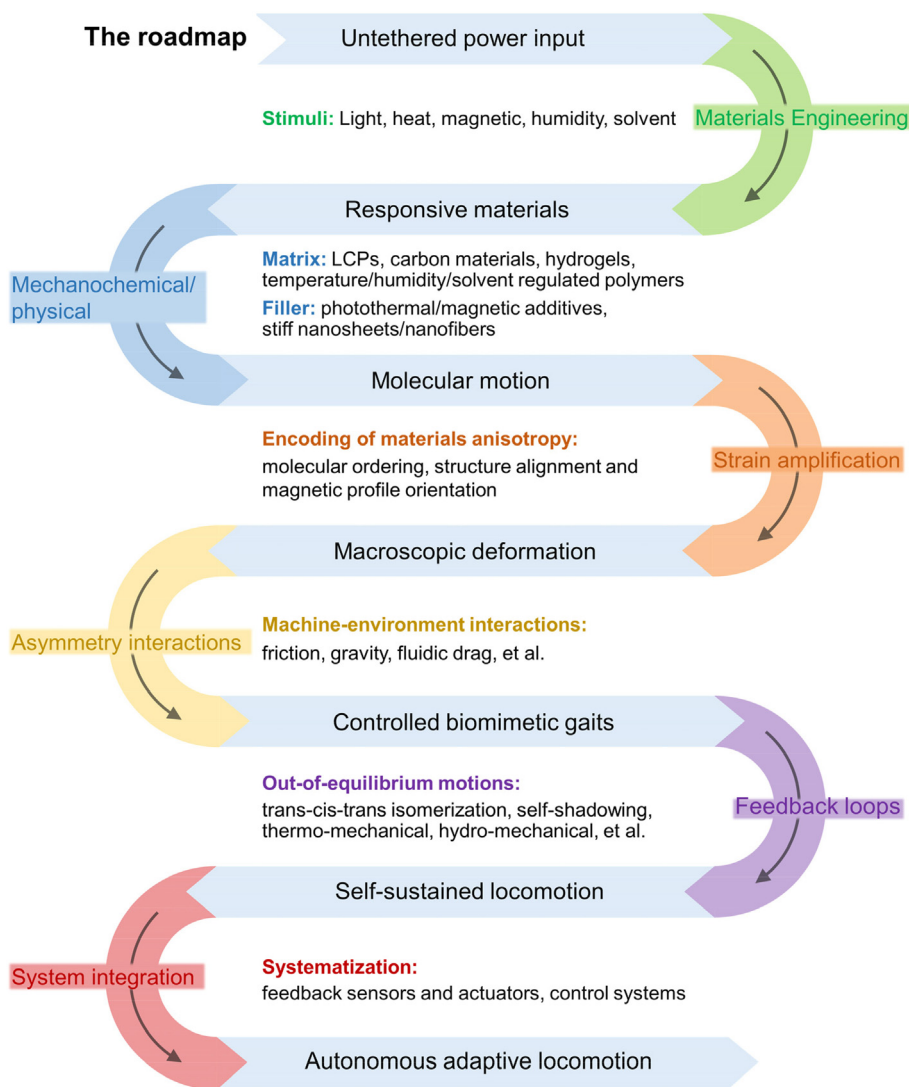
to contortion of cells, microorganisms and animal bodies and their interactions with the environment to produce various untethered locomotion. We also examine several feedback loop mechanisms that are inspired by the biological out-of-equilibrium principle [39] to realize autonomous behaviors in soft micromachines, which follow specific environmental cues. And we finally review the most recent progress at robotic shaping, morphing, assembly and system-level integration of sensors and actuators for proficient locomotion and advanced functionalities.

## Materials and micromachine engineering

Smart and compliant materials are the building blocks of soft micromachines, and their chemistry, physics and engineering are the central endeavors of the current research efforts. Here, several representative soft systems coupled with their machine engineering principles are capable of performing swift actuation in Fig. 2. The machine engineering refers to material design principle and engineering that enables the device to deliver directed or programmed motions in response to specified stimuli, similar to many tools and machines used in our daily life [40,41]. The active responsiveness of materials facilitates the transduction of input energy into relevant molecular shape changes/motions, while the harnessing of molecular changes by multi-mechanism design across the molecular to the centimeter scale enables their amplification into various macroscopic deformation. Fast and reversible shape transformations are emphasized, which are of paramount importance to support agile life-like locomotion. The production, amplification and regulation of mechanical strain for controlled deformation based on tactical material systems, energy sources and engineering strategies are the primary focus. The advantages/disadvantages of each kind of micromachine system toward locomotion purpose are also discussed.

### *Molecular ordering in crosslinked liquid-crystal polymer*

Crosslinked liquid-crystal polymers (CLCPs) are well-shaped polymer systems with ordered molecular alignment of the liquid crystals, including liquid-crystal elastomers (LCEs), polymer networks (LCNs), and gels (LCGs) [42,43]. Stimuli-responsiveness of CLCPs are based on the self-assembly property of liquid crystalline molecules or mesogens and cross-linking of polymers. In CLCPs, the conformation of polymer chains is strongly coupled to the alignment of mesogens [44]. The subtle reduction in ordering of the mesogens can introduce molecular forces to the cross-linked polymer chains and cause conformation changes, thereby producing mechanical strain of the polymer networks. As a result, the macroscopic shape can be directly related to the alignment of mesogens and the shape transformation of a CLCP system is governed by the order-disorder phase transition of the mesogens (Fig. 2i), which are triggered by external stimuli [45–49]. The presence of cross-links in polymers, in turn, ensures that the initial ordering state is recoverable after removal of the energy source. A reduction of the mesogen ordering from the aligned state causes contraction of polymer chains along the alignment direction (director) and expansion in the other two perpendicular directions. Consequently, a full nematic-to-

**FIGURE 1**

A general roadmap toward the design of untethered soft material machines with life-like locomotion.

isotropic transition will generate a large contraction strain along the director, enabling in-plane contraction deformation, while the different in-plane expansion/contraction along the thickness direction of a CLCP beam actuator is exploited for producing large out-of-plane bending deformation.

The order–disorder phase change can be driven by photochemical effect (Fig. 2ii) or thermal/photothermal effect (Fig. 2iii). Photochemical actuation is based on photoswitchable molecules, such as azobenzenes [50], diarylethenes [51] and spiropyran derivatives [52], which experience reversible shape changes upon photon absorption. Azobenzene derivatives are the most popular photoswitches in LCPs, owing to the distinct advantages such as ease of synthesis and compatibility with many liquid crystalline molecules. In azobenzene-based LCPs (azo-LCPs), the azobenzenes are covalently bonded to the polymer network, and undergo trans–cis isomerization upon irradiation with ultraviolet (UV) or deep blue light. The rod-like trans-isomers stabilize the liquid crystalline phases, whereas cis-isomers perturb the molecular alignment, causing shape defor-

mations. The initial liquid crystalline is recovered through thermal back cis–trans isomerization when exposed to light irradiation of 450–550 nm. Particularly, the photochemical effect relies on light absorption gradients over the thickness direction of a CLCP sample. In an azo-LCP system with high concentration of azobenzenes, most of the incident light is absorbed near the surface [46,53]. An azo-LCP film with planar nematic alignment will bend toward the incident light as illustrated in Fig. 2ii. Thermotropic LCEs are able to undergo fast phase transition near the nematic–isotropic transition temperature ( $T_{ni}$ ) [54], thereby generating large, powerful, and repeatable deformations when subjected to direct heating/cooling processes. In a thermal LCE actuator, temperature rapidly equilibrates across the whole sample, whereby planar alignment specimen gives rise to a large contraction deformation while splay-alignment as illustrated in Fig. 2iii facilitates a large bending deformation toward the planar-oriented side. To enable efficient and remote control of temperature changes in LCEs, photothermal agents, such as organic dyes [55,56], carbon nanotubes (CNTs) [57,58] and gold

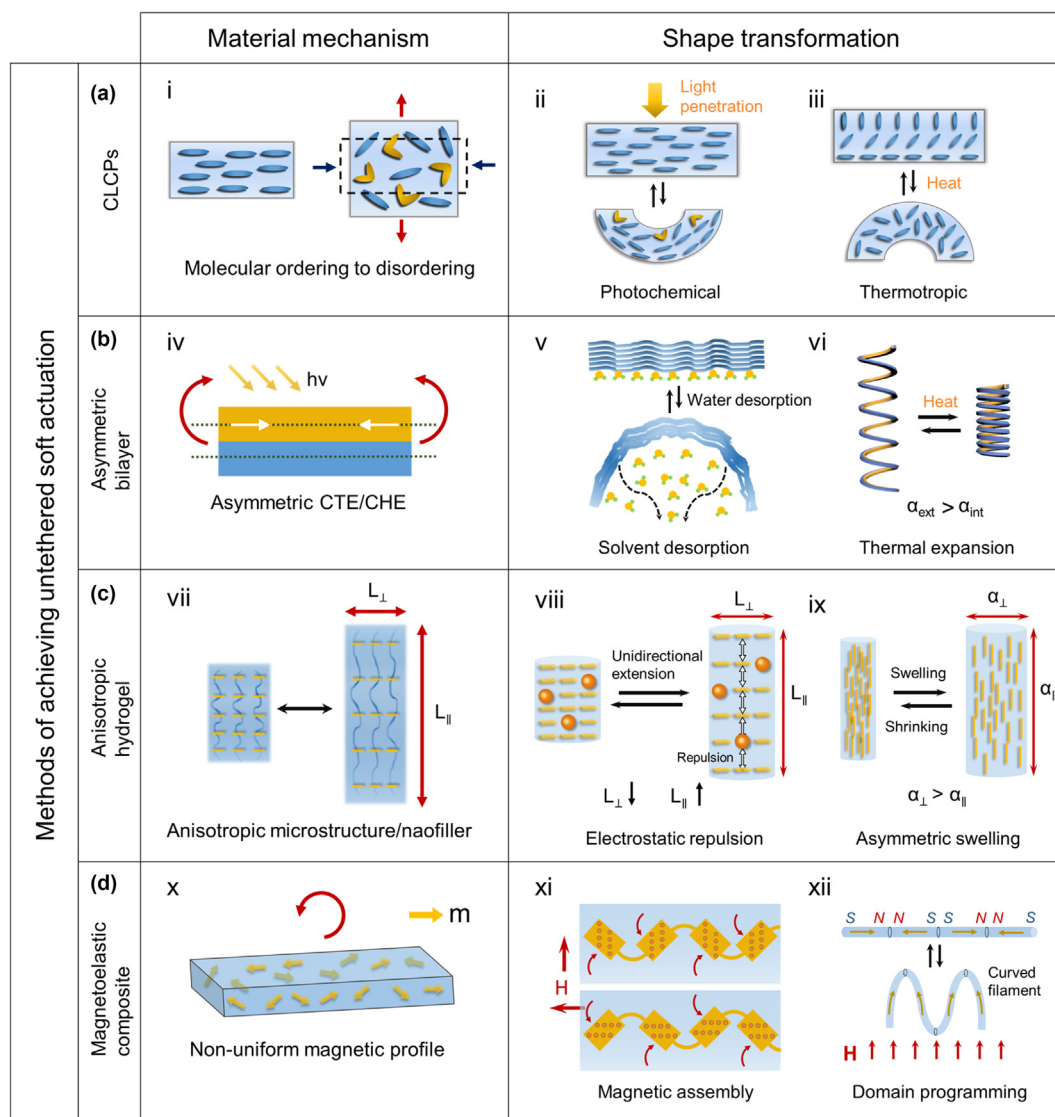


FIGURE 2

Material mechanisms and machine engineering strategies to achieve various deformations of different soft material systems. (a) Crosslinked liquid-crystal polymers (CLCPs). (i) Disordering of mesogens in CLCP. (ii) Directed light induced deformation of an azo-LCP film with planar alignment. (iii) Shape change of thermotropic LCEs with splayed alignment triggered by heat. (b) Asymmetric bilayer. (iv) Bilayer structure with asymmetric CTE or CHE. (v) Bending deformation of GO-PDA/rGO bilayer film induced by water desorption [144]. (vi) Linear actuation of helical bilayer with mismatched CTE. (c) Anisotropic hydrogel. (vii) Anisotropic deformation of hydrogels with orderly aligned nanofillers or microstructures. (viii) Unidirectional extension of PNIPAM hydrogel with cofacially oriented titania nanosheets [122]. (ix) Anisotropic swelling of a hydrogel filament with aligned cellulose fibrils [114]. (d) Magnetoelastic composite. (x) Non-uniform magnetic profile in the soft matrix. (xi) Shape transformation of a soft actuator with anisotropic alignment of superparamagnetic nanoparticles [138]. (xii) Deformation of a soft filament with programmed ferromagnetic domains [142].

nanoparticles [59], are usually added to the LCE material system. Depending on the heat capacity, photothermal LCEs are able to rapidly deform within milliseconds to seconds. Unlike that of azo-LCPs, the direction of photothermal induced deformation such as bending is independent of light irradiation site. By proper selection of photothermal agents, LCEs can be actuated across the whole visible-near infrared spectrum, acceding photothermal effect to biological applications where ultraviolet light should be avoided.

Notably, there is large scope for engineering diverse initial shapes or complex two-dimensional to three-dimensional (2D to 3D) shape transformations by programming the molecular orientation along the thickness [60–62] or 2D surface directions of

CLCP actuators [63–65], which is an ongoing active research topic in the field of CLCP materials. What makes CLCP unique is the design freedom to encode complex deformation modes in a single CLCP system by programming the molecular alignment. This attribute would allow the design and seamless assembly of diverse deformations capable CLCP units to create multitask capable soft micromachine models [66,67]. Compared to photochemical actuation, thermal/photothermal actuation of LCEs is considered to be more suitable for driving continuous locomotion because of their fast relaxation times. While photochemical actuation is promising to function well in an aqueous environment due to its heat conduction independence, and the long lifetime of cis-isomer in azo-LCPs is likely to enrich

the functionality of locomotion by the shape memory effect based on the photoisomerization [68].

### Asymmetric bimorph

Isotropic single active material always exhibits homogeneous variation in volume when subjected to a uniform external stimulus, such as thermal expansion in response to an increased temperature and solvent absorption induced swelling. However, in a film-like device with asymmetric property along the thickness direction, a modest difference in volume change, can drive a large bending deformation. As such, a small in-plane mechanical strain is transformed into a large macroscopic out-of-plane bending deformation [69,70]. This principle has been widely used for construction of various soft actuators responsive to light, heat, humidity and solvent, applicable to a broad range of active materials. Typically, a bimorph actuator composed of two materials with different coefficient of thermal expansion (CTE), bends under a thermal/photothermal stimulus (Fig. 2iv). The deformation behavior is predictable based on the Timoshenko beam theory [69]. In a bimorph thermal actuator, materials with large contrast in CTE are usually combined for producing large deformation. Some common polymers with large positive CTE include polydimethylsiloxane (PDMS), polyvinylidene fluoride (PVDF), biaxially oriented polypropylene (BOPP) and polycarbonate (PC), while materials with low or negative CTE comprise papers, carbon nanotubes (CNTs) and graphenes [27]. Thermotropic LCEs are used as the thermal active layers in bimorph actuators as they undergo phase change induced expansion/shrinking [71]. Owing to the excellent light-to-heat conversion property, CNTs and graphenes are often incorporated into thermal active matrix to facilitate efficient light control. Moreover, they can also work as independent layers due to their high mechanical strength. A hygroscopic polymer or responsive hydrogel layer is usually combined with another passive material layer, thus forming a bimorph actuator responsive to humidity and volatile solvent vapor. These humidity-responsive materials with high coefficient of hygroscopic expansion (CHE) [72,73], mostly contain hydrophilic groups such as hydroxyl, carboxyl, amide, or pyrrolyl, typical examples being GO [74], cellulose [75,76], MXene ( $\text{Ti}_3\text{C}_2\text{T}_x$ ) [77,78] and metal-organic frameworks (MOFs) [79]. As illustrated in Fig. 2v, a bilayer actuator consisting of polydopamine modified GO (GO-PDA) in rich of water molecules and reduced GO (rGO), bends toward the GO-PDA side when the NIR light irradiation induces water desorption, and upon light off, shape recovery materializes with humidity absorption. Besides, thermal responsive poly(N-isopropylacrylamide) (PNIPAM) hydrogel possesses a reversible shrinking-swelling phase transition at its lower critical solution temperature (LCST,  $\sim 32^\circ\text{C}$ ) [80]. Hence, PNIPAM hydrogel and their related materials are frequently combined with another passive layer, such as GO [81], elastomers [82], and temperature-inert hydrogels [83] to support reversible shape transformation in aqueous environment. Additionally, it is worth mentioning that asymmetry along the thickness direction can be achieved not only by stacking distinct bi-materials, but also by devising gradient properties in a single-layer material [84–87]. Aside, out-of-plane shape transformation of a single-layer active material without gradient properties could

also take place if localized or directional external stimulus is exerted at the selective area [88,89].

Chirality-creating mechanism in natural plants inspires design of multimodal shape change of bilayer actuators beyond the primary bending deformation. The multimodal shape changes include rolling, coiling, and twisting, achieved by various molecular alignment or microchannel structure in polymers [90–92], alignment of CNTs [93], and orientation of hydrogel fibers strategies [94]. A prestrained method is applied to create bilayer actuators with helical shapes [95], allowing thermal tensile actuation along the length direction of the helix. If CTE of external layer is larger than the internal layer ( $\alpha_{\text{ext}} > \alpha_{\text{int}}$ ), the helical bilayer coil shortens in the length direction when it is heated as illustrated in Fig. 2vi. Besides, patterning of hydrogel on a 2D surface to create local and different response by methods, such as photopatterning [96], ion-printing [97] and ion-transfer-printing techniques [98] can realize complex or programmed deformations. Recently, the kirigami/origami technique has been applied to customize the shape of bilayer actuators [99,100], generating diverse 2D-to-3D shape transformations.

Asymmetric bimorph concept is a general principle, which embraces a huge diversity of the materials library. Many active materials are commercially available or easy to synthesize, holding promises for scalable production of soft mobile micromachines. However, the limitation lies in structural engineering. For instance, if two materials with distinct properties are to be laminated, materials interfacing may pose a problem. In this case, different interfacial bonding strategies, such as physical attachment [95], covalent bonding [101] and interfacial percolation [102] should be adopted to fabricate robust bimorph structures that tolerate repeated and various shape transformations. Depending on different combinations of functional materials, the resultant mobile micromachines could have vast difference in mechanical strength, actuation speed and deformation extent properties. In addition, compared to the single-layer design of LCP micromachines, the bimorph principle with open material systems favorably allows more room for engineering multiple responsiveness into one soft machine capable of synchronous built-in functions (self-sensing [103], sensing of external signals [83,104] and energy generation [105,106]) along with actuation.

### Microstructure ordering in hydrogel

Of all the solid-state materials, gels can achieve the largest volume change [10]. When heated above its LCST, PNIPAM hydrogel is able to transform from a swollen state to a shrunken state with a volume change of 90% [107]. Besides bending, curling and twisting, the contraction/expansion motion has widely been developed in the animal kingdom, such as the tentacles of snail, the body of earthworm and the tube feet of starfish. In these cases, an intrinsic uniaxial large actuation strain is required for a unidirectional contraction/expansion, different from the out-of-plane bending deformation based on the bimorph principle that utilizes a small in-plane strain. The hydrogels are considered as the most promising candidates for such a purpose, due to the capability of large volumetric variation [108–110]. However, common hydrogel actuators without specific structural design are isotropic with omnidirectional activity. They exhibit volu-

metric change uniformly in all directions, hence making them unsuitable for a uniaxial actuation, i.e. a reversible displacement in one specific direction. To deal with this problem, internal ordering of microstructures in hydrogels to create anisotropic mechanical response [111], proves to be an efficient method, as illustrated in Fig. 2vii. The microstructural ordering can transpire as alignment of polymer molecular chains [112,113], ordering of 1D- or 2D-shaped nanofillers such as cellulose fibers [114], carbon nanotubes [115], GO [116] and inorganic nanosheets [117,118], or orientation of channel-like microscale pores [119,120]. Correspondingly, responsive hydrogels with ordered microstructures are able to deliver anisotropic volume change or even unidirectional actuation deformation. For instance, upon heating (45 °C), a cylindrical PEG-PNIPAm hybrid hydrogel with aligned pores shrunken by 50% in the direction perpendicular to the channels, while experiencing negligible shrinkage in the axial direction [121]. And remarkably, a PNIPAM hydrogel with cofacially oriented titania nanosheets reversibly expanded by 170% within 1.5 s in the length direction by means of an abrupt electrostatic repulsion between the nanosheets upon thermal stimulus [122]. And Fig. 2viii schematically illustrates the isochoric deformation process, which does not involve water uptake or release. Besides, hydrogel embedded with aligned cellulose fibrils had a fourfold longitudinal and transverse swelling strains of  $\alpha_{\parallel} \sim 10\%$  and  $\alpha_{\perp} \sim 40\%$ , respectively (Fig. 2ix), and programming of the hydrogel architectures with ordered microstructures allowed versatile and complex shape changes [114,123,124]. Recent development of novel microstructure ordering techniques, such as shearing microlithography [125] and shear-flow-induced alignment [126] will open up more opportunities for programming the anisotropy of responsive hydrogel machines. Typical hydrogel actuation based on the swelling and de-swelling process is usually slow and requires the presence of water environment. To enable fast reversible deformation for locomotion in an aqueous environment, new structural designs of the hydrogel materials as well as novel actuation principles are imperative. Meanwhile, hydrogel dehydration restricts its stable and repeated stimulus-responsive operations in the air. To keep stable water retention of hydrogel actuators in air, strategies such as encoding moisturizing factors in hydrogels or encapsulation using elastomers can be applied [127].

#### *Anisotropic magnetization in magnetoelastic composites*

Materials producing strain in response to magnetic fields are known as magnetoelastic materials [128]. In a soft composite with finely distributed magnetic particles, the conformation change of polymer chains is strongly associated to the response of the magnetic particles under magnetic field influence. Compared with polymer composites attached with individual rigid magnets, magnetic particles incorporated soft composites provide a fully soft body, continuous magnetization profile, and adeptness at complex deformation and locomotion. Different magnetic materials, including superparamagnetic, paramagnetic, and ferromagnetic particles with length scales of nanometers to micrometers have been used [129–132], while the typical soft matrices are passive elastomers [133,134], gels [135] or stimuli-responsive gels [136]. Isotropic magnetoelastic composites experience no strain in a uniform magnetic field. Whilst magnetic

translational force and torque can be generated if subjected to a magnetic field gradient or a rotated magnetic field, thus feasibly triggering contraction, bending or rotation motion [129,137]. However, engineering anisotropic magnetization profile in magnetoelastic composites, such as programming particle alignment [138,139], magnetic polarity [3,140] and distributed magnetization [141] allows design of more complex deformations. Instant shape transformation of the actuator in response to fast magnetic fields variations could possibly generate multimodal locomotion. As illustrated in Fig. 2x, non-uniform magnetization profile,  $m$  with controlled directions can be defined in a soft matrix for generating complex deformation via the magnetoelastic effect. For example, Kwon and co-workers first created anisotropic alignment of superparamagnetic nanoparticles in photocurable resin by the magnetic field induced assembly followed by photopolymerization at different parts of the composite liquid resin [138]. A microactuator containing four different magnetic axes exhibited reconfigurable bending in different angles under a uniform magnetic field line (Fig. 2xi). Alternatively, it is feasible to magnetize embedded ferromagnetic neodymium-iron-boron (NdFeB) particles after the soft composites are cured as proposed by Sitti and co-workers [140]. By 3D printing an elastomeric ink containing NdFeB microparticles, Zhao and co-workers were able to program ferromagnetic domains in various 3D soft structures (Fig. 2xii) [142], and complex shape changes and locomotion such as jumping, crawling, and rolling under magnetic fields can be designed. In conjunction with the kirigami/origami technique, the magnetization approach has recently manifested various biomimetic models design and multiple reconfigurable shape-morphing [143]. Taken together, soft magnetoelastic micromachines are promising in delivering high mobility and agile locomotion in virtue of fast and diverse shape transformations in response to varying magnetic fields.

#### **Controlled locomotion for biomimetic gaits**

Moving beyond the soft material engineering for actuation strategies, the key question is how to harness the shape deformation to build untethered mobile machines, i.e. transform the shape change into directional displacement of the center of mass (COM). This requires a step forward proceeding from structural asymmetry in machines to asymmetry of the interactions with the surroundings. Symmetry deformation oscillation can be rectified into directional locomotion by engineering asymmetry interactions between the mobile body and its environment. Alternatively, the asymmetry can also be achieved when a mobile machine changes its body shape in a manner that is non-reciprocal. The dynamics are quite different for locomotion in a dry environment and a liquid medium. Progressive understanding of various propulsion strategies of the biological counterparts, has advanced the development of biomimetic soft robotic locomotion in complex environment.

#### *Legged and limbless crawling*

Terrestrial locomotion of animals has inspired designs of various biomimetic gaits in untethered soft machines. In the biological gaits, periodic pulses of muscular deformation are rectified by one or more symmetry-breaking mechanisms, resulting in fric-

tion dominated propelling on land [145,146]. And the asymmetric interaction involved in mobile artificial machines can be incorporated by engineering (i) the material structure and properties, (ii) the body shape or (iii) the shape of deformation pulse.

In a typical beam robot model generating periodic bending/unbending deformation, friction bias at the two ends of the beam is required for a directional inchworm-like locomotion. And anisotropic frictional force can be introduced by engineering a ratcheted substrate to make forward movement easier during bending/unbending cycles [147–149], whereas such a locomotion strategy relies on the specific substrate characteristics, resulting in limited mobility. In contrast, friction bias that is directly implanted in specific robot legs/feet allows multi-terrain agility [4,150–154]. In this regard, Kim and co-workers fabricated a legged hygrobot, i.e. a ratcheted bimorph actuator responsive to humidity change, which was able to generate directional locomotion on flat surfaces [152]. The legs at the two ends rectified the humidity fluctuation induced bending-unbending oscillations into directional movements. In this way, a typical inching locomotion mode was realized (Fig. 3a). Two-way or multidirectional inching movement can be engineered by triggering localized body deformation in soft robots. For example, two-way walking was performed by a bilayer LCE film of which one layer was a polydomain LCE ribbon without mechanical

alignment and another layer was a head-to-head joint of two uniaxial-stretched monodomain alignment LCE ribbons doped with different photothermal organic dyes. The right and left parts along the body length direction of the prepared LCE walker bent under the 808 and 980 nm NIR irradiation respectively (Fig. 3b) [66]. Upon 808 nm NIR light on/off, the right side bent and bulged to produce a larger friction than the left side, and pushed the inchworm leftward. In a similar way, the LCE walker would move rightward under repeated on/off cycles of 980 nm NIR light. Recently, Stupp and co-workers reported a cross-shaped photoactive spiropyran (SP) hydrogel film containing nematic order dispersed ferromagnetic nickel nanowires (left of Fig. 3c). Upon exposure to directed visible light, the gradient of hydrophobic SP moieties along the thickness direction of the flat hydrogel film would be induced, and the light-exposed side with a high density of SP expelled water, leading to bending toward the incident light. Meanwhile, bent geometry of the hydrogel deformed the existing magnetization profiles to produce complex 3D magnetization that enabled programmable deformation of the soft body. Under rotated magnetic fields, the object landed on its front and back legs in alternating fashion to walk and steer, and the two longer side arms with a larger magnetic torque were important in stabilizing the hydrogel's movement and optimizing its lift during walking (right of Fig. 3c) [155]. Instead of inch-

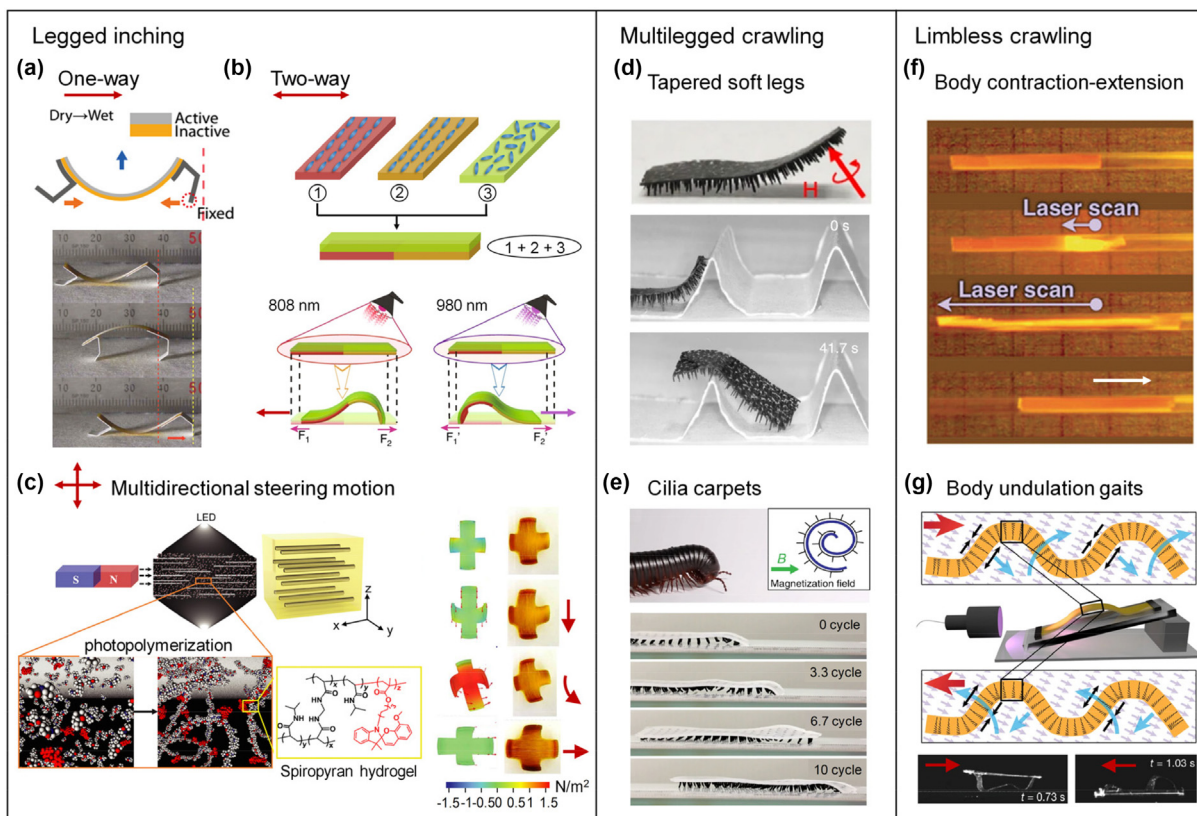


**FIGURE 3**

Biomimetic walking gaits in untethered soft machines including legged inching, multilegged crawling and limbless crawling. (a) Directional inching of a hygrobot with ratcheted legs [152]. (b) NIR dual-wavelength modulated two-way inching of a bilayer LCE walker [66]. (c) Steered movement of a cross-shaped hydrogel film under rotating magnetic fields and light illumination [155]. (d) Crawling and climbing of a soft magnetic millirobot with multiple tapered soft legs [159]. (e) Millipede-inspired crawling of a magnetic cilia carpet [160]. (f) Earthworm-like directed peristaltic crawling of an anisotropic hydrogel actuator [165]. (g) Undulating LCP walker utilizing out-of-plane deformation waves of its body [167].

ing locomotion seen in small slender caterpillars, crawling is a common gait in larger caterpillars, which involves a wave progression of muscular activity from the posterior body segments toward the head [156–158]. Wasylczyk and co-workers designed a caterpillar-like robot made from a LCE strip with alternately patterned alignment. By scanning a laser beam from the tail to the robot's head, curly bending deformation travelled along the body, allowing it to climb a slope or squeeze through a slit [157].

Myriapods, animals with multiple legs or feet achieve their land crawling locomotion mainly by the exertion of soft leg muscle deformation rather than the change of body length. Shen and co-workers reported a soft magnetic millirobot decorated with multiple tapered soft legs [159]. The tapered soft feet containing aligned magnetic particles were deformed and aligned with magnetic flux and when a magnetic bar was moved up and forward, the forebody was raised and moved forward step by step. The tapered soft legs significantly reduced body friction, and made the locomotion efficient on both wet and dry surface. And the resilient deformation of the soft legs gave rise to superior ability to overcome obstacles, allowing the multi-legged robot to climb and cross steep obstacles (Fig. 3d). In another example, non-reciprocal motion of the travelling metachronal waves was generated in the artificial magnetic cilia carpet by a clockwise rotating magnetic field, and drove the carpet to perform the millipede-like crawling (Fig. 3e) [160].

In addition to the legged crawling, limbless animals, such as earthworms, snakes, and snails, possess various intriguing body deformation waves to propel themselves without legs or feet. In the peristaltic crawling locomotion, the earthworm alternatively contracts and extends its body segments, generating rectilinear locomotion along its body axis [146,161–164]. This peristaltic crawling mechanism requires very limited amount of space, especially suitable for locomotion in tightly confined terrains when legged motion fails. Aida and co-workers created an entirely soft hydrogel robot that exhibited earthworm-like peristaltic crawling under a spatiotemporal light control [165]. The anisotropic composite hydrogel consisted of PNIPAM matrix filled with electrostatic charged cofacially oriented titania nanosheets and photothermal gold nanoparticles. As shown in Fig. 3f, the forebody became longer and thinner under laser irradiation, generating reduced friction with the capillary wall that facilitated forward extension. As the irradiation spot moved gradually to the end of hind body, the forward contraction of the hind body occurred as the thick forebody was in tight contact with the capillary wall. In such a way, the hydrogel continuously crawled forward. Similarly, peristaltic crawling was also mimicked by thermotropic LCE machines, in which contraction-extension motion travelled along the body in a single alignment under the thermal/photothermal stimulus [166]. Besides, Broer and co-workers demonstrated photoactuated deformation waves in an azo-LCP film, which locomoted in a way analogous to the lateral undulation gaits of snakes. Azobenzene derivatives with fast cis-to-trans thermal relaxation were incorporated into the liquid-crystal networks, allowing continuous, directional mechanical waves in the LCP film under constant ultraviolet light illumination, with a feedback loop driven by self-shadowing. The locomotive device consisted of a LCP film in

splay alignment attached to a plastic frame (Fig. 3g). As the out-of-plane deformation waves in the LCP film continuously travelled along the body, a part of its body periodically contacted and pushed the ground backward, and therefore generated a propulsive friction for directional movement [167].

### Wheel-like rolling

Some animals can actively transform into wheel-like shape to perform high-speed escapes in certain environment. Typical wheel-like motions examples are ballistic rolling of Mother-of-pearl caterpillar, backward somersaults of *Nannosquilla decemspinosa*, and downhill rolling of Namib Golden Wheel Spider [168]. Wheel-like dynamics have also been exploited for untethered soft micromachines, in which light, heat, humidity or a rotated magnetic field generated torque is utilized to actively drive a rotary locomotion. In a circular soft device, shape deformation induced by the external stimulus results in a change of the geometric COM, thereby driving rolling motion along the desired direction [78,169–172]. This design principle is often applied to the design of wheel-like soft rolling machines, such as the fast forward-moving SWCNT/polycarbonate bimorph motor driven by visible light [169], the azo-LCP/BOPP soft wheel directed by UV light [171], the humidity powered GO/chitosan composite motor [172], and the fast flipping long polymer crystal plate triggered by temperature gradient [173]. Chen and co-workers devised a graphene/PE bimorph roll by creating residual elongation in the graphene layer of a flat graphene/PE bimorph film via a constrained tempering process. Upon lateral IR illumination on the left side of the bimorph roll, the outmost layer of the roll unfolded, flattened, and interacted with the ground to propel a forward rolling. When the outmost layer of the roll moved to the right side, its temperature dropped due to the displaced IR illumination. Hence, the outmost layer returned to its initial curled status, generating a restoring momentum [174]. In such a way, the roll would continuously move forward (Fig. 4a). Besides, winding-unwinding shape transition of helical ribbons was utilized to generate a torque to drive rotation of wheels [171]. Beyond these linear rolling forward motion of wheel-like machines, a kirigami-based legged LCP rolling machine was reported, which was tubular in shape with active side petals capable of steering the rolling direction [175]. Under visible light irradiation, the splay-aligned LCP petals incorporated with photothermal dye (Dispersed Red 1) bent toward the substrate, and lifted up and tilted COM of the soft machine, thus leading to rolling locomotion. By controlling the light direction, different petals could be actuated that made the soft machine turn left/right, roll forward, or other desired paths (Fig. 4b). Under clockwise rotating magnetic fields, a tubular magnetized soft magnetic composite equipped with stick-shaped legs was demonstrated not only capable of moving on dry and flat land, but also able to transport a cargo amidst various terrains, including wet land, leaves land, and sandy and stony lands (Fig. 4c) [176]. Additionally, Ho and co-workers demonstrated a self-shaping roll that performed self-propelled rolling motion, which was sought to mimic the biological self-defensive process [105]. Upon placing onto a hot surface of  $\sim 70^\circ\text{C}$ , the original thermal responsive flat polydopamine modified reduced graphene oxide-carbon nanotube/PVDF (PDG-CNT/PVDF) bimorph plate bent

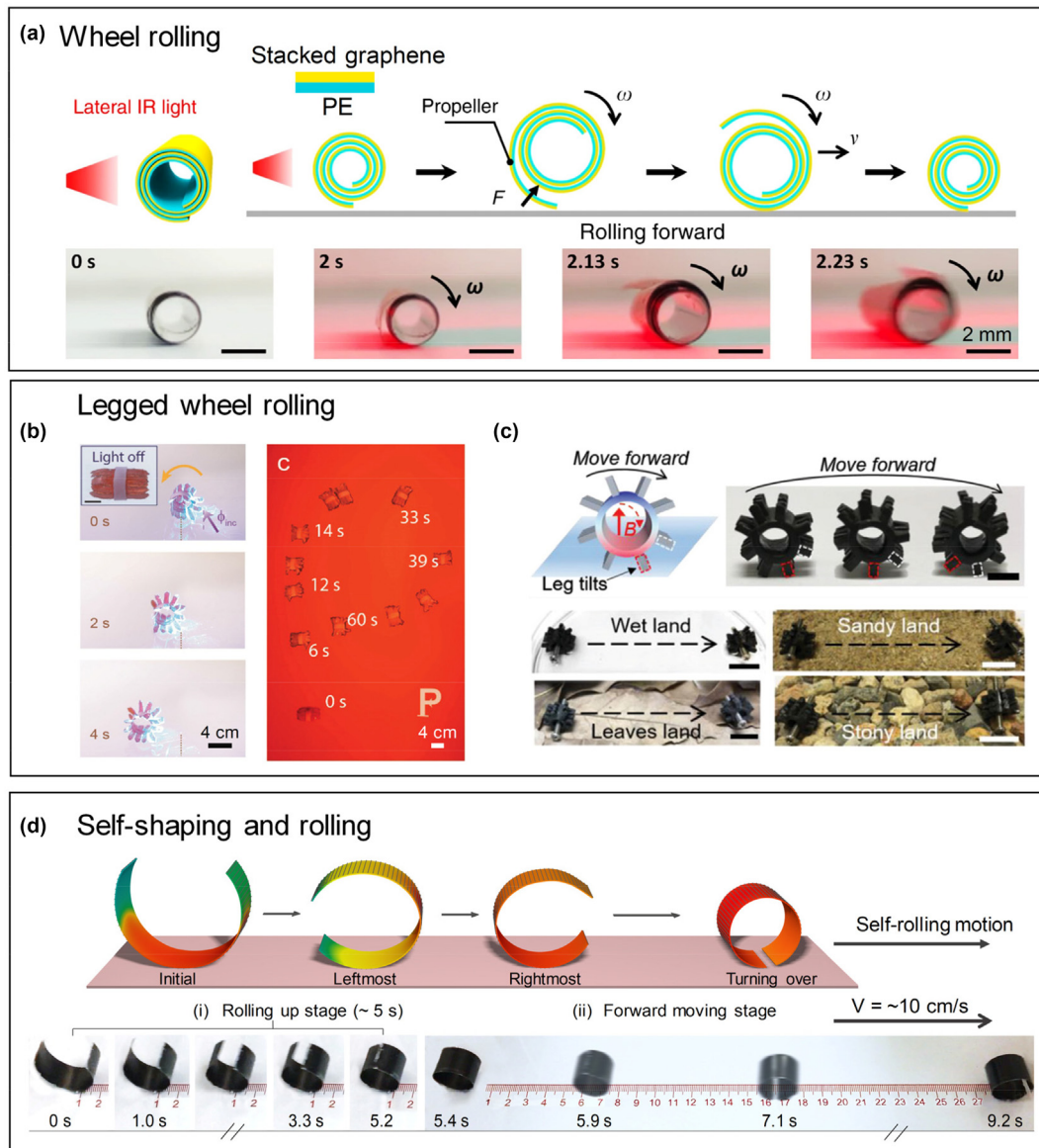


FIGURE 4

Wheel-like rolling of soft micromachines. (a) Lateral IR light illumination induced rolling locomotion of a graphene/PE bimorph roll [174]. (b) Steered rolling motion of a kirigami-based legged LCP rolling machine [175]. (c) Forward moving wheel-like magnetic robot carrying a cargo on various terrains [176]. (d) Self-shaping and rolling motion of a PDG-CNT/PVDF bimorph on a hot surface [105].

rapidly, and oscillated perpetually. Along with the oscillation process, temperature gradient in the bimorph plate gradually decreased, and the plate gradually evolved into a circular shape and rolled forward at a speed reaching 10 cm/s (Fig. 4d). This response is akin to the ballistic rolling response of caterpillars, i.e. dynamic body morphing into a wheel-like shape under an emergency plight followed by a fast rolling escape [177,178].

#### Legless jumping

Compared with crawling or rolling, jumping is a fast and efficient way for small robots to get around obstacles [179,180]. Jumping and hopping are most often achieved with legs, but jumping mechanisms that do not involve legs are seen in some small animals, such as the body hinge torque in inverted click beetles [181], terrestrial tail-flip in bony fishes [182], and latching

and hydrostatic manipulation in insect larvae [183]. By utilizing different body maneuvering strategies, all the biological legless jumpers strive to accomplish a power amplification mechanism, which is crucial to achieving high acceleration. The process typically engages body latching in allowing elastic energy loading over an extended period, and a subsequent fast release of stored energy, thus reaching a high acceleration and uplifting of the body into the air. Deployment of this general biological principle into small mobile machines, has enabled legless jumping locomotion without any special appendages. The reported small untethered soft jumpers were mostly powered by light, heat or magnetic fields [3,142,150,184–190]. For example, an anisotropic carbon nitride polymer (CNP) film with asymmetry along the thickness direction, curled up within 50 ms due to its instant water desorption upon UV light irradiation. Owing to its ultra-

light weight (10  $\mu\text{g}$ ) and nearly instant actuation, the flat CNP film could jump vertically up to 10 mm, 5 times its body length (BL) when photoirradiated [185]. Recently, Wie and co-workers designed an azo-LCN with liquid crystalline monomers arranged in a molecular spring-like 270° super twisted nematic (STN) geometry, which had bi-stable structures and performed jumping motion via snap-through upon 365 nm UV light exposure with substrate heating (Fig. 5a) [191]. The maximum jumping height reached 15.5 BL with an instantaneous velocity of 880 BL  $\text{s}^{-1}$ , and the direction of jumping was controlled by exerting top-down or bottom-up light beam irradiations with different beam profiles. A latched tubular bimorph jumper fueled by simulated sunlight was also designed [186]. Thermal curing of the CNT/PDMS bilayer generated thermal stress at the interface, leading to rolling and latching of the two ends of the bilayer when the temperature decreased to the room temperature. After  $\sim 3$  s light irradiation, the latch instantly released to lift the body up to 32 mm, about 5 times its own height. Besides, magnetic control allows better maneuverability of the soft bodies. Millimetre-scale magnetoelastic machines with programmed magnetization profile were able to jump along a desired direction under controlled magnetic fields [3]. The magnetic torque enabled clockwise rotation of the body in a 'C'-shape bending configuration (0–13.5 ms), and as the ends of the robot hit the ground under the constant magnetic field (13.5 ms), a power amplification process

was completed, enabling the robot to instantly jump to the right (Fig. 5b). Straight jumping was realized by devising a magnetic machine with symmetrical magnetization profile along the body length direction. Recently, a hydrogel jumper composed of a binary iron oxide nanoparticle (IONP, i.e.  $\text{Fe}_3\text{O}_4$  NP) and poly (sodium acrylate) (PAANA) hydrogel composite was designed by utilizing the synergetic interactions between the elasticity of the hydrogel sphere ( $\sim 1$  mm-radius) and the gas bubble caused by photothermal effect of the embedded IONP [192]. Under light irradiation at the bottom of the hydrogel ball, photothermal effect of IONPs triggered the gasification of water and formation of bubble inside the hydrogel. The fast expanding local protrusion hit the substrate and drove the jumping of the hydrogel ball (Fig. 5ci). An ultrafast take-off speed of around 1.6  $\text{m s}^{-1}$  and a superior jumping height of 15 cm with fast response time of only 800 ms under 2.34 W irradiation was recorded, and the jumping directions were controlled by adjusting the irradiation positions (Fig. 5cii).

### Swimming

Swimming is a locomotion in a liquid medium with directional forward motion regulated by shape deformations, fluid forces, and their interactions [193,194]. For a swimmer with a characteristic size of  $d$ , moving at speed  $v$  in a fluid with density  $\rho$  and viscosity  $\mu$ , the Reynolds number  $\text{Re} = \rho v d / \mu$  gives the ratio of

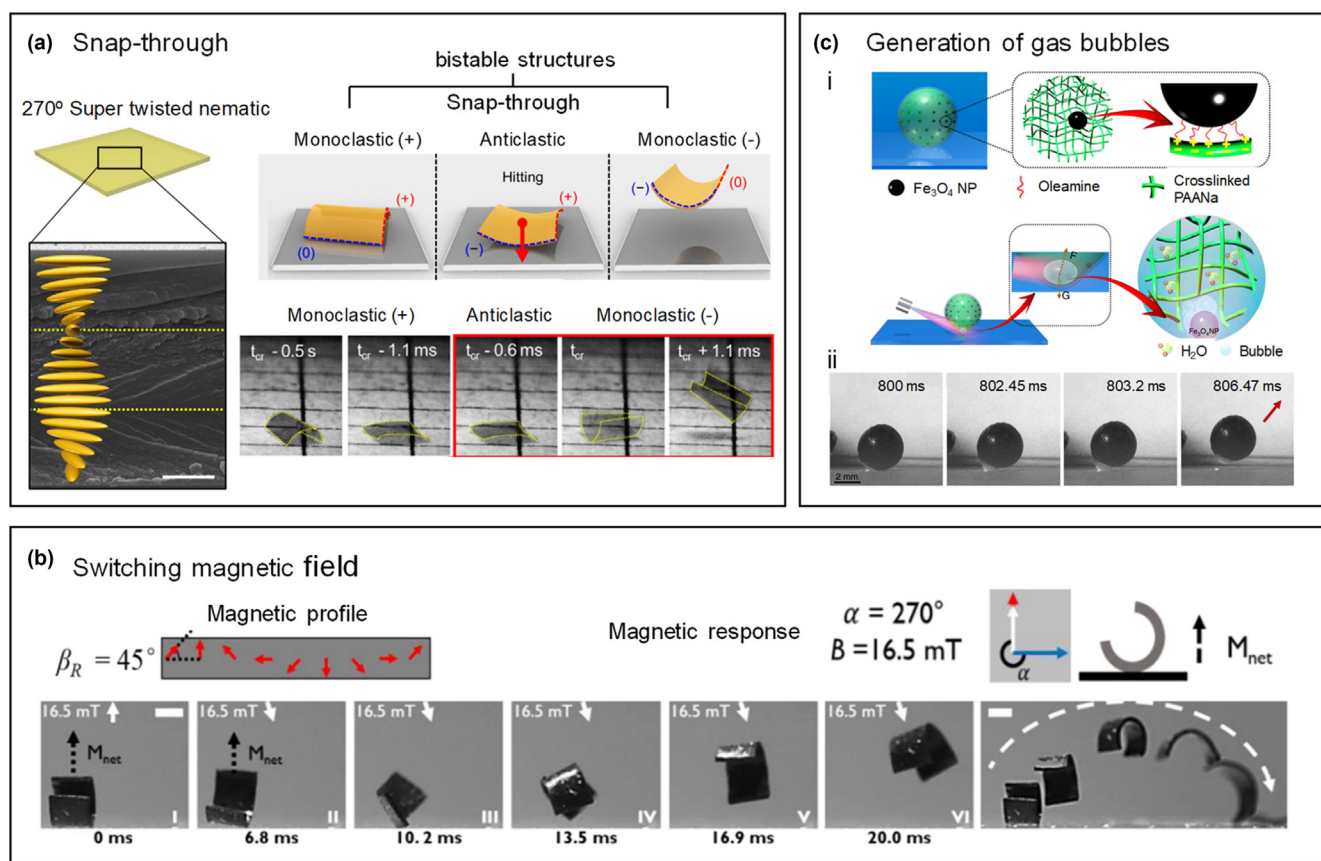


**FIGURE 5**

Legless and directed jumping based on different power amplification mechanisms. (a) Jumping of an azo-LCN film with molecular spring like super twisted nematic alignment via snap-through [191]. (b) Jumping of a millimeter magnetic robot via fast switching of the magnetic field [3]. (c) Jumping of an elastic hydrogel ball triggered by generating gas bubbles via photothermal effect [192].

inertial to viscous forces. In water,  $Re$  is about  $10^5$  for human swimmers, 1–10 for small fishes and  $10^{-5}$  for bacteria [195]. Qualitatively, moving in liquids is dominated by inertial forces for large  $Re$ , and when the  $Re$  is small in micrometer scale organisms and machines, viscous forces govern the motion while inertial forces are negligible. For  $Re \ll 1$ , the flow of a liquid is described by the time-independent Stokes equation, which implies that the flow is instantaneous and time reversible. As a consequence, ‘the scallop theorem’ of Newtonian fluids, such as water, a geometrically perfect reciprocal motion that proceeds in shape changes that are identical when reversed, cannot achieve a net propulsion [194]. Therefore, non-reciprocal shape transformation becomes the center of current research efforts to develop soft microswimmers. In recent years, the non-reciprocal propulsive strategies of swimming microorganisms and cells have aroused great interest. It has advanced the development of propulsion strategies, including the corkscrew-like propulsions owing to rotation-translation coupling inspired by the bacterium *Escherichia coli* [196,197], bending waves of flexible filaments like in spermatozoa cell [198], and travelling wave synchronized motion as observed for ciliate protozoa [199].

So far, externally controlled artificial soft microswimmers are often driven by magnetic fields. Helical micropropellers are effective solution for the propulsion of micromachines in water. While realization of rotary motors at the microscale is not easy, and the artificial microswimmers inspired by the helical bacterial flagella are typically driven by external rotating magnetic fields [200–203]. Forward and backward corkscrew propulsion of magnetic helical micropropellers is readily controlled by changing the direction of magnetic-field rotation (clockwise or counterclockwise), and the propulsion speed strongly depends on the helical shape [204]. Besides, Möller and co-workers reported the propulsion of helical PNIPAM microgel embedded with gold nanorods, which was enabled by nonequilibrium actuation/shape change via plasmonic heating [205]. Propulsion of a typical sperm inspired the head–tail robot consisting of a magnetic head with a flexible tail, to perform passive and planar beating/bending of the flexible tail under magnetic torques [206–208]. Nelson and co-workers fabricated soft micromachines comprising of a magnetized tubular head and a thin flexible tail [206]. The anisotropic swelling of poly (ethylene glycol) diacrylate-PNIPAM hydrogel bimorph structure and the alignment of magnetic nanoparticles in the hydrogel layers, were utilized to program the body shapes and magnetic anisotropy of the 3D biomimetic microswimmers. Under a rotating magnetic field at low frequencies, the micromachine with a planar tail or a helical tail could move forward due to the head–tail coupling (Fig. 6a), while a larger precession angle led to superior swimming performance in the planar tail. At high rotating frequencies, corkscrew propulsion mode in helical tail would be activated, facilitating reversible propulsion directions. Propulsion enabled by propagation of bending waves found in sperm cell or ciliate protozoa can be mimicked by the magnetoelastic composite machine with distributed magnetization [141,209]. A millimeter-sized flexible composite sheet with programmed magnetization profile along the body length direction reacted to a rotating magnetic field with a continuous transverse wave, and propelled itself at a constant speed on the water surface or underwater (Fig. 6b) [140].

Besides, propulsion by travelling waves of radial expansion and longitudinal contraction was realized in LCE swimmers using a structured light field [210].

Unlike the microrobot under the millimeter scale, an artificial swimmer with size comparable to a small fish experiences medium Reynolds numbers in water. In this case, both inertial and viscous forces play significant roles in the dynamics of aquatic locomotion, and ‘the scallop theorem’ does not apply. As indicated by ichthyologists, the propulsion strategies fall into two categories according to the body parts that are utilized to generate thrust: body and/or caudal fin (BCF) propulsion, and median and/or paired fin (MPF) propulsion [211]. Besides, the jellyfish has a jet propulsion swimming mode [212]. Fish-like aquatic locomotion can be realized by using smart actuators as the oscillation fins or undulatory bodies. And typical biomimetic robotic fishes were usually not fully soft and electrically powered, such as using the ionic polymer metal composites (IMPCs) [213], piezoelectric actuator [213,214] and dielectric-elastomer actuators (DEAs) [215,216]. Recently, Sitti and co-workers reported jellyfish-inspired soft millirobots that beat up and down its eight lappets in a non-reciprocal manner powered by oscillating magnetic fields [217]. By analyzing the fluidic flows around its body under controlled contraction and recovery strokes, the jellyfish-like swimming mechanics in Reynolds number ( $Re = 7\text{--}95$ ) similar to an ephyra were carefully studied (Fig. 6c). And the fluidic flows were further regulated for predation-inspired object manipulation tasks. Additionally, body propulsions of simple and fully soft material systems via oscillation bending were also reported [86,218,219]. For example, a splay-aligned LCG construct was successfully actuated in an underwater environment via the photothermal effect, and the resulting light-induced buoyancy ( $F_B$ ) and the propulsive thrust ( $F_T$ ) led to upward swimming motion of the LCG construct in a symmetrical bending deformation (Fig. 6d) [220]. And a thermal responsive hydrogel strip with gradient porosity bent under a localized NIR laser irradiation that facilitated forward movement on the water surface [86].

### Out-of-equilibrium autonomous motion

Robotic actuation and locomotion are typically generated and sustained by dynamic change of stimulus, such as intensity changing, rotating or cyclic on–off magnetic fields on magnetoelastic composites, and using AC signals on piezoelectric actuators. Thus, these locomotion mechanisms involve complicated external control and/or human manipulation of energy sources. In contrast, living organisms can directly harvest energy from a constant/unchanged environment and generate autonomous and continuous oscillation motions, a few examples being cell cycling, heartbeats, and neuron impulses [39]. Those biological systems mostly possess unique out-of-equilibrium properties deriving from their built-in feedback loops, which support dynamic interaction of two or more kinetically stable states. If these out-of-equilibrium mechanisms could be built into soft robotic systems, it would be extremely advantageous for realizing untethered autonomous robots, which respond to the different environmental cues to perform ceaseless and directional self-propelling movement.

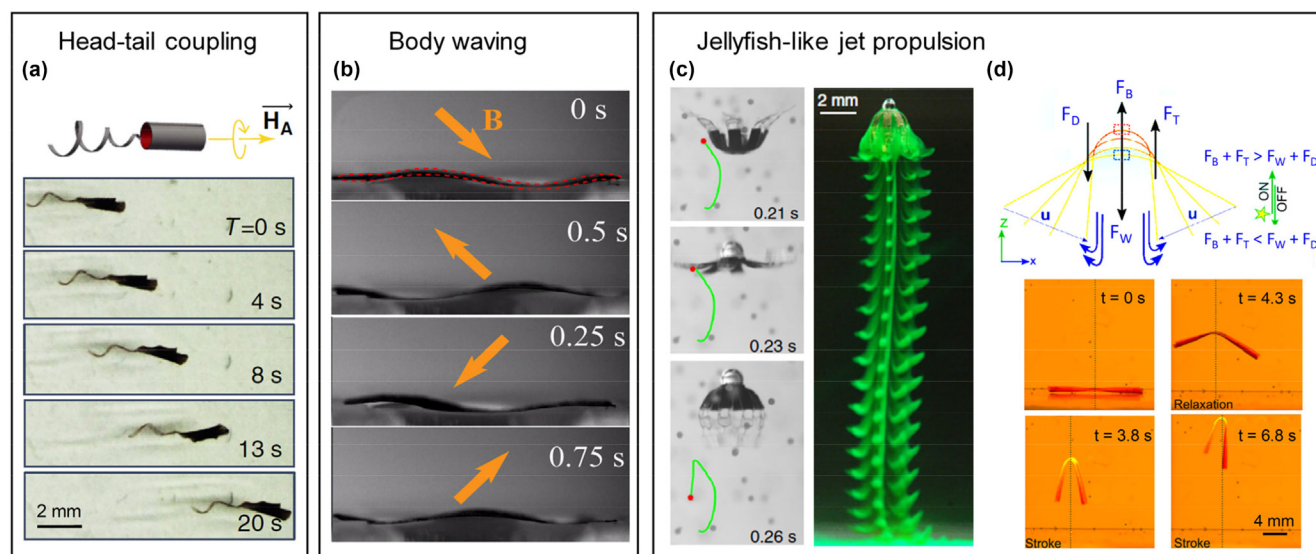


FIGURE 6

Locomotion strategies of soft machines in a liquid medium. (a) The forward swimming of the flagellated soft micromachine under rotating magnetic fields [206]. (b) Travelling body wave of a flexible composite sheet with programmed magnetization profile [140]. (c) Jellyfish-shaped soft millirobots beating up and down its eight lappets in a non-reciprocal manner powered by oscillating magnetic fields [217]. (d) The upward motion of a splay-aligned LCG construct in underwater environment actuated by light illumination [220].

### Self-oscillation

Autonomous oscillations are characteristic of living matters, while engineering rational feedback loops would likely implement out-of-equilibrium actuation in artificial active systems, to conceivably achieve continuous, perpetual oscillation under an unchanging, constant energy source. In recent years, encouraging progress has been made in this emerging field, and several novel oscillation mechanisms are introduced into different soft material systems, including chemo-mechanical oscillation based on the Belousov-Zhabotinsky reaction [221], chemo-mechanochemical self-regulation [222], *trans-cis-trans* isomerization [223], self-shadowing [167], thermo-mechanical oscillation [105], and humidity or solvent vapour driven mechanical oscillation [224]. The feedback loop mechanisms that are powered by light, heat, humidity and solvent vapour will be elaborated in this section. In principle, all these feedback loops are constructed by the interplay between the equilibrium position upon stimulus and responsive deformation of the device.

The oscillation mechanisms involved in LCPs can be mainly classified into *trans-cis-trans* isomerization [225–229] and self-shadowing [56,230,231], primarily driven by the photochemical and photothermal effect, respectively. It was reported that an azo-LCP cantilever in nematic alignment self-oscillated under a laser beam excitation, prompting upward-downward flapping motions. During this process, the laser alternatively hit on the two surfaces, and thus *trans-cis-trans* isomerization occurred sequentially on the two surfaces to induce cyclic upward-downward bending deformation with the maximum oscillation frequency of  $\sim 30$  Hz (left of Fig. 7a) [223]. Instead of the photochemical isomerization of the mesogens driven oscillation, Yang and co-workers designed a LCN oscillator triggered by dynamic photochemical isomerization of molecular motors. Reversible stable-unstable isomerization of the overcrowded alkene motor

with trifunctional acrylate groups in the LCN framework resulted in photodynamic storage modulus in the local UV light exposure areas of the actuator (right of Fig. 7a) [232]. Based on modulation of spatial photodynamic modulus of the LCN film, chaotic or regular oscillations were regulated by controlling the loading contents of the molecular motors in the LCN and the intensity of UV light. As for the photothermal effect, a light spot hit on a LCP film generated bending deformation, which then shadowed the original irradiation area, in turn resulting in a temperature drop and unbending of the film to the original position [56]. The oscillation was sustained by the self-shadowing effect, which was also applied to other soft material systems, such as the light-powered bimorph actuators [106,233,234] and hydrogels [235]. In a recent work, a helical graphene doped LCE fiber actuator was devised for a phototunable self-oscillating system (PSOS). The oscillation system consisted of the straightened helical LCE fiber under loading, which tended to recover the original helical shape under NIR irradiation irradiation due to the photothermal induced phase transition of the mesogens. During this process, the width of the NIR light spot irradiated on the LCE fiber must be smaller than the diameter of the coils, that is to say, the light induced coils of the LCE fiber need to be partially out of the light spot to enable a self-shadowing effect. Oscillation modes including tilt oscillation, rotational oscillation, and up-and-down oscillation were switchable by changing the position and width of the NIR light beam (Fig. 7b) [236]. These light-driven self-oscillating devices based on LCPs were mostly fixed at one end, allowing high oscillation frequencies but limiting their application toward mobile and locomotive soft machines.

In this aspect, Ho and co-workers proposed a free-standing film oscillating device on a hot surface based on a thermo-mechanical feedback loop, capable of multimodal oscillations and waste heat ( $<100$  °C) harvesting. The thermo-mechano-

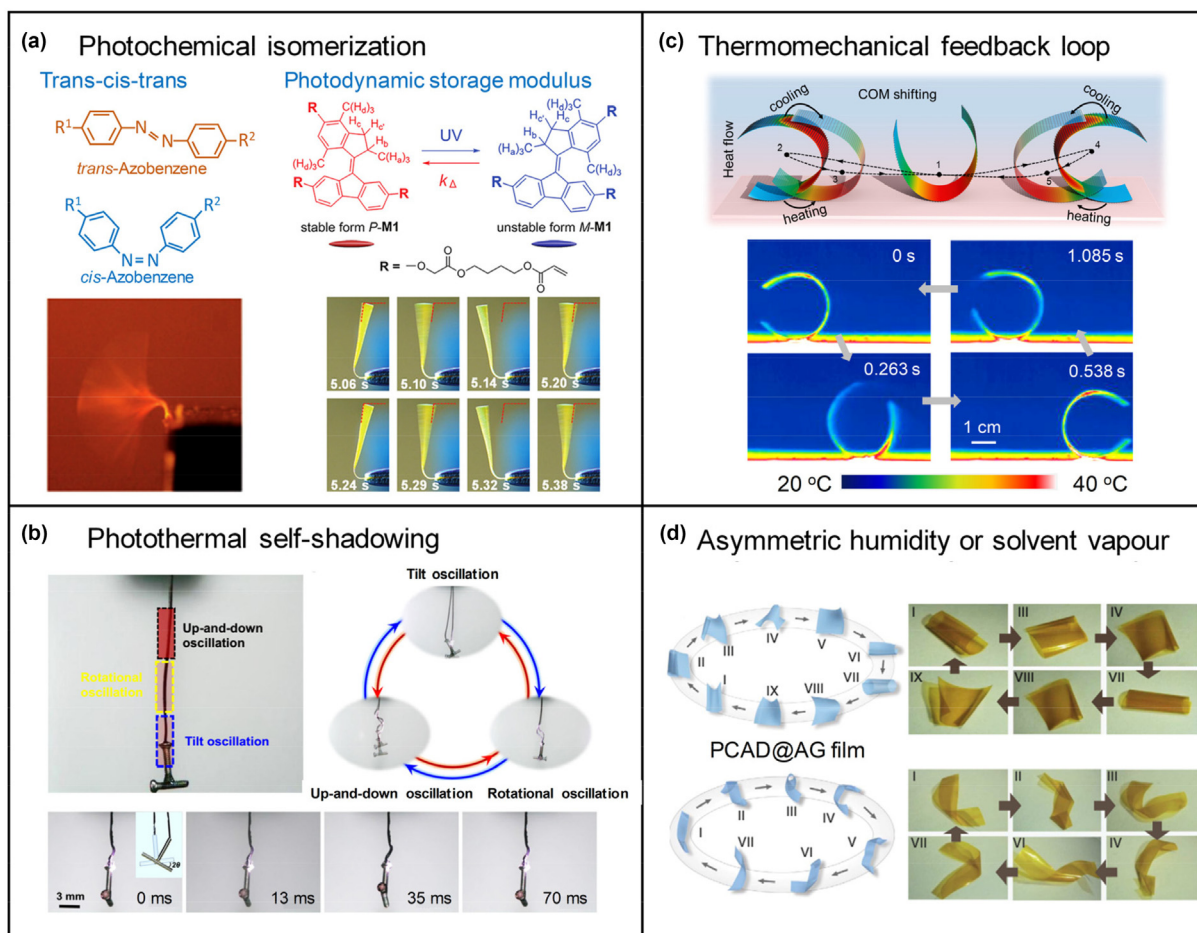


FIGURE 7

Self-oscillation motions sustained by various feedback loop mechanisms. (a) Upward-downward flapping motion of azo-LCP cantilever in nematic alignment under excitation with a laser beam (left) [225] and self-oscillating of the LCN incorporated with an overcrowded alkene motor based on photodynamic modulus (right) [232]. (b) Diverse oscillatory motions of a photoactive self-winding fiber actuator via the photothermal self-shadowing effect [236]. (c) Self-oscillation of the bimorph actuator on the hot surface via the thermomechanical feedback loop [105]. (d) Locomotion of humidity responsive composite films on a moist substrate [237].

electrical system (TMES) bent symmetrically on the hot surface based on the thermal bimorph principle. Upon reaching a large deformation at a temperature above 55 °C, the device lost its balance and oscillated to the leftmost position. Then the left side of the device in contact with the hot surface was heated up while the right side exposed to air was cooled down, resulting in inclination of its COM to the right, and thus the device oscillated to the right. Due to the motion inertia, the device continuously oscillated to the rightmost, and then similar heating/cooling effects to that of the leftmost position made the device oscillate to the left again (Fig. 7c) [105]. As this behavior was repeated, cyclic oscillation happened. Specifically, the built-in ferroelectric property of the device enabled simultaneous harvesting of the thermo-mechanical energy for electricity generation, thereby forming a unique thermo-mechano-electrical energy conversion path. Besides, humidity or solvent vapour driven oscillation could proceed with a thin single-layer active film that was exposed to asymmetric humidity or solvent vapour distribution [73,224,237–239]. For example, a flipping oscillation of a humidity active pentaerythritol ethoxylate-polypyrrole composite film on a moist surface was demonstrated. The water gradient

between the substrate and air induced a curling deformation, as the bottom face of the film in contact with the substrate absorbed more water. The curling deformation then raised the gravity center of the film, facilitating toppling over motion. After it flipped over, a new face of the film contacted the moist surface, and thus initiated a new cycle. This film could carry a cargo 10 times heavier than itself to oscillate on the moist surface, and generate electricity when associated with a piezoelectric element [224]. Guided by similar interplay mechanisms, a poly(ethylene glycol)-conjugated azobenzene derivatives@agarose (PDAG@AG) composite film delivered periodic shape reconfiguration with a turnover frequency of  $\sim 150 \text{ min}^{-1}$  on the moist surface, and the active film with different aspect ratios would undergo different modes locomotions (Fig. 7d) [237].

#### Directional self-propelled movement

Beyond the self-oscillation behavior, an onward progress is to fabricate untethered mobile machines capable of continuous and directional locomotion, which follow specific environmental cues. And this poses more challenges, as it requires not only out-of-equilibrium actuation to drive continuum motions, but

also symmetry breaking motion to generate adequate propulsive forces that overcome the friction or fluidic drag. A few pioneering examples have shed light on this prospect, and shaped our primary understanding of the self-propelling behaviors viable on the ground or in the water [62,105,235,240–247]. A rotary engine was devised by assembling humidity responsive spore-polyimide bimorph film actuators around two concentric rings, and small blocks of acrylic were attached at the free ends of the actuators to increase the torque. Half of the actuators were exposed to a high humidity enclosure, and thus the humidity difference between the humid enclosure and the outside dry air resulted in bending-unbending oscillations of the actuators. And the cyclic horizontal shift in COM of the entire structure created torque that sustained the rotational motion, which was utilized to drive a wheeled car (Fig. 8a) [241]. This design strategy highlights the utility of water evaporation into the atmosphere to power automatic machines. Self-propelling movements dictated by a specific thermal environment have also been exploited in recent years. Kulić and co-workers proposed a model, termed the ‘embedded wheel’, which allowed self-propulsion of polymer fibers on a hot surface [242]. A straight fiber was subjected to a temperature gradient between the hot plate and the surrounding colder air, and the resulting bending deformation stayed in-plane. Meanwhile, the curved fiber was still exposed to the temperature gradient, causing another thermal strain in the direction normal to the plane. The combined effect led to a dynamic instability, and created a torque driving the rolling motion, in typical speeds of centimeters per second. Under this model, the direction of the torque and the rolling velocity depend on the positive or negative polarity of the CTE. In another example, Lewis and co-workers printed a structure that self-folded into a pentagonal prism and rolled forward on a hot surface, which was termed the

‘rollbot’. The origami inspired structure had two kinds of active LCE hinges, including low  $T_{ni}$  ( $LT_{ni}$ ) hinges and high  $T_{ni}$  ( $HT_{ni}$ ) hinge that became fully isotropic at 92 °C and 127 °C, respectively. On the hot surface at round 200 °C, a large torque produced by bending deformation of the  $LT_{ni}$  hinges enabled folding of the flat structure into a pentagonal prism. The  $HT_{ni}$  hinges bent/unbent when in/off contact with the hot surface, and produced a torque that drove forward rolling, therefore sustaining repeated actuation and continuous locomotion (Fig. 8b) [244]. Directional locomotion of an azo-LCN under a light illumination was demonstrated by White and co-workers. A flat film of twisted-nematic alignment on the surface responded to the top-down UV-visible light illumination with a spiralled deformation, and then rolling forward motion. The impulse in the spiral geometry with asymmetry between the light irradiated and shadowed regions resulted in a net torque. And when combined with the substrate friction, generated a momentum that shifted the COM of the spiral and led to a rolling motion under the continuous and constant light irradiation. The rolling direction and speed were controlled by changing the angle between the nematic director and the spiral’s long axis, as well as the light intensity (Fig. 8c) [62]. In addition, self-propelled phototactic swimming was reported by He and co-workers, who developed gold nanoparticles incorporated PNIPAM photothermal responsive hydrogel self-oscillating in water, fueled by a constant visible light illumination [235]. The oscillation mechanism was rooted on the photothermal self-shadowing effect coupled with the high-speed actuation. Directional propulsion of a biomimetic swimmer was generated by using the hydrogel oscillator as its caudal fin, and the swimmer was able to propel itself away from the light source with a maximum speed of 1.15 BL  $\text{min}^{-1}$  (Fig. 8d).

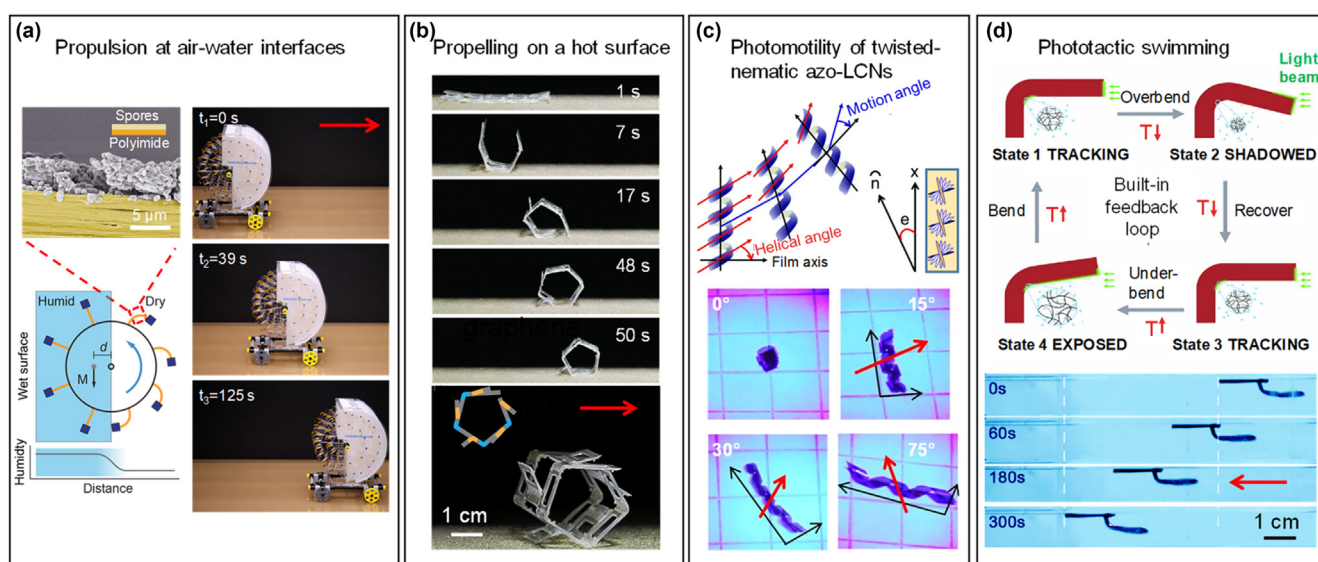


**FIGURE 8**

Self-propelling motions proceeded in different scenarios. (a) Forward motion driven by continuous rotation of a rotary engine powered by evaporation from the wet paper within the device [241]. (b) Self-propelling of an origami inspired ‘rollbot’ on a hot surface [244]. (c) Directional and continuous locomotion of a spiralled azo-LCN film in twisted-nematic alignment under the light illumination [62]. (d) Soft phototactic swimming based on the self-sustained hydrogel oscillator [235].

## Adaptive and sensory locomotion

Living matters constitute of integrated sensory and actuator systems, with exceptionally rich capabilities, such as motility, sensation, protection, predation, etc. To go beyond the current level of motility sophistication, future efforts on biomimetic soft machines will focus on improving the locomotion adaptivity and mastery of advanced functionalities, in order to allow robots to operate in complex environment and perform elaborate tasks, such as object manipulation [248–250], drug delivery and release [251,252], camouflage [7,253–255], proprioception to real-time sensing of body kinematics [256], and exteroception to perceive the environment [257], etc. This endeavor will require research into integrated material and device systems as well as rational interplay between various mechanisms. As discussed, the untethered locomotion strategies of soft micromachines are largely determined by the on-board sensors, i.e. the responsiveness to external energy sources. In this part, we provide a brief discussion on the recent progress of technologies promising for advancing the locomotion adaptivity and sensing capability of untethered soft micromachines.

### Reconfigurable shape morphing and modular assembling/disassembly

To increase the locomotion capability and adaptivity in a complex environment, i.e. to locomote on different terrains, negotiate obstacles, navigate in confined spaces, and move in a fluidic environment, the soft machine should have sophisticated capa-

bilities to rapidly reconfigure its body shapes and master multi-modal actuation/locomotion modes. So far, magnetoelastic soft robots with programmed magnetization profiles have exhibited remarkably agile shape morphing under controlled magnetic fields. Under different torques induced by time-varying magnetic fields, a millirobot of the single-wavelength harmonic magnetization profile in a simple rectangular-sheet shape was deformed into sine and cosine shapes to produce travelling wave along the body under small magnetic fields, and deformed into ‘C’ and ‘V’ shapes to enable rolling, walking and jumping under high magnetic fields [3]. By utilizing the capability of swiftly manipulating body shapes, the millirobot was able to locomote in various modes and transit reversibly between different liquid and solid terrains. Recently, Sitti and co-workers further proposed the locomotion control of sheet-shaped soft millirobots in fluid-filled confined spaces. In such complex situations, body-environment interactions affected by the surrounding boundaries, the hydrodynamic and frictional forces, and the robot’s active soft-bodied deformation must be well controlled. And they proposed optimal body deformation and locomotion modes in different fluid-filled confined environment, such as straight/bent gaps with varying sizes, tortuous channels, and tubes with a flowing fluid (Fig. 9a) [258]. Engineering multimaterials integrated architectures is another promising way to elaborate shape morphing of soft micromachines [259–262]. For example, a hydrogel with multiple DNA-cross-linked domains, fabricated using photolithography process, exhibited pro-

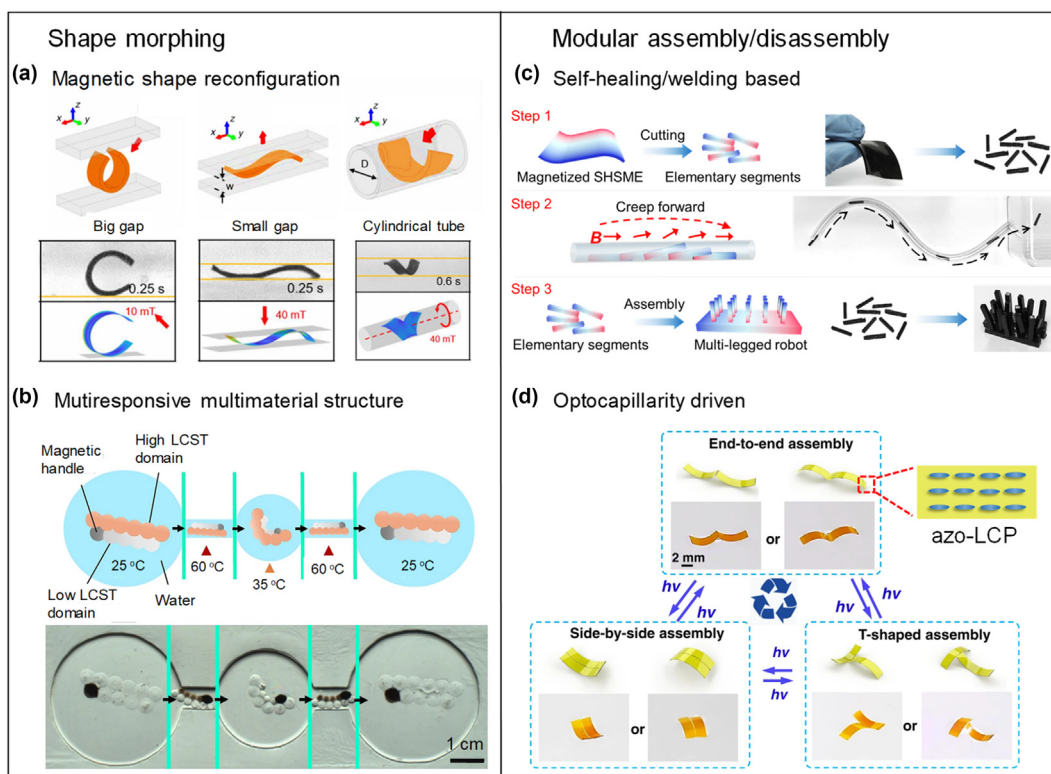


**FIGURE 9**

Shape morphing and modular assembling of soft machines in complex environment. (a) Adaptive body deformations of the magnetic millirobot in different fluid-filled confined spaces [258]. (b) Multi-responsive shape-changing hydrogel structure [262]. (c) Dismembering-navigation-assembly strategy of the self-healing soft robot for navigation of a confined and curved space [176]. (d) Optocapillarity-driven assembly and reconfiguration of azo-LCP films on the liquid surface [265].

grammable shape changes to DNA sequence [259]. Also a multi-material 3D printing method has been utilized for manufacturing a combustion-powered soft robot that performs multiple jumps [260]. Recently, a droplet network technology was introduced by Bayley and co-workers, for patterning of multi-responsive domains into a hydrogel on a micrometer to millimeter scale. A patterned hydrogel composed of temperature-responsive domains, gold nanoparticle-containing domains and magnetic particle-containing domains, could locally respond to different stimuli, including temperature, light and magnetic fields [262]. High locomotion adaptivity and cargo transport capability were demonstrated. The hydrogel machine shrank at a high temperature, allowing it to pass through a 500- $\mu\text{m}$ -diameter channel under the magnetic field control, and it re-swelled and curled due to the anisotropic swelling at a lower temperature (Fig. 9b). Based on this principle, a multi-responsive hydrogel gripper was able to navigate a maze, and transport a cargo droplet.

Reversible assembly/disassembly of small building modules could alternatively fulfill reconfigurable designs of soft robots capable of adjusting their shapes/morphologies to adapt to multiple tasks. Different methods such as welding [67,263], self-healing [176,264] and capillary force induced assembly [265], have been recently reported for the reconfiguration of untethered soft robots. For example, by welding and aligning LCE materials, multimaterial LCE soft machines possessed different chemical compositions and physical properties at different parts of the body, and displayed complicated 3D machine- and animal-mimicking actuation [67]. Ho and co-workers recently introduced a fast, self-healing supramolecular magnetic elastomer (SHSME). The damaged magnetic robot could recover its locomotion ability within 5 s self-healing on the ground or underwater, facilitating rapid amphibious function recovery. By utilizing the high mechanical strength and fast self-healing capability of the robot, they conceptualized a dismembering-navigating-assembly strategy for robotic tasking in confined spaces. Upon encountering a tortuous and narrow channel with a dimension that exceeded the robot body, a bulk magnetized material was able to dismember into elementary segments to pass through the channel successively, and subsequently assembled remotely and self-healed at ambient into desired 3D architectures via noncontact magnetic assembly (Fig. 9c) [176]. Aside, capillary interactions are usually exploited to assemble objects with specific shapes into ordered structures on the liquid surface, whereas dynamic tuning of capillary interactions to achieve programmable assembly and reconfiguration of floating systems is rarely seen. Recently, the optocapillarity induced by reversible photodeformation of floating azo-LCP films was utilized to realize assembly and reconfiguration of actuators across multiple fluid interfaces. UV irradiation can induce directional bending (positive/negative curvatures) of the flat azo-LCP film with ordered mesogens while visible light can make the film unbend and return to the flat state. End-to-end, side-by-side and 'T' shapes were assembled and reconfigured by reversibly deforming the azo-LCP films into bending states of positive/negative curvatures (Fig. 9d), allowing floating objects to develop complex morphology reconfiguration [265]. This strategy provides a way to

fulfill reconfigurable designs of swarm robots in liquid environment.

### *Somatosensory feedback and environment exploration*

Despite the tethering issues, introducing electronic sensor networks into soft machines would enable robots to precisely express their sophisticated perceptions using digital readout signals, such as haptic [257,266], proprioceptive [103,256,267–272], and thermoceptive sensing [100,273]. These functions are of great value for the next generation of intelligent soft mobile machines that seek to be aware of their own motion states and surrounding environmental situations, thus achieving more adept and purposeful locomotion. However, building sensors and actuators in one soft micromachine for synergetic functions remains challenging. For example, the accuracy of the sensing signals can be interfered by many factors, such as the power sources that drive the actuation (light, heat, humidity or magnetic fields), and the deformation states of the robot. The actuation performance of the micromachine may also be degraded by the implantation of sensors. Creative material and structural designs on the sensors and actuators are required to engineer robotic intelligence. In this regard, Ho and co-workers reported a smart thin-film composite that compactly integrated a pyroelectric temperature sensor, a piezoresistive strain sensor and a bimorph photothermal actuator. The robotic functions including body temperature sensing, deformation sensing and light-driven actuation were simultaneous and non-interfering. This thin-film robot performed light-driven locomotion, while providing real-time piezoelectric resistance change and pyroelectric voltage signals that precisely conveyed its body motion state and temperature, respectively [100]. Arbitrary biomimetic robot prototypes could be rapidly customized and easily downsized via the kirigami technique. When equipped with a near-field communication (NFC) chip, an untethered centipede-like robot, was able to crawl forward, turn, and wirelessly sense light intensity, wind speed and human touch (top of Fig. 10a). A robotic walker provided feedback on its detailed locomotive gaits and the subtle terrain textures when it walked on different surfaces (bottom of Fig. 10a). In another work, multilayers of the piezoelectric film, electrodes and multi-legged soft magnetic composites were assembled together to couple magnetic actuation and piezoelectric effect. Under the same magnetic actuation condition, the millirobot delivered identifiable time-dependent piezoelectric voltage waveforms at different interfaces, including the flat rigid interface, stagewise rigid interface, stagewise soft interface and liquid interface (Fig. 10b). Besides, they offered an additional carried-on thermistor that could sense temperature changes when the moving millirobot was exposed to an infrared light illumination [273]. Recently, an ice templated constitution followed by UV- and cryo-polymerization (ITUC) of the polyaniline (PAni) and PNIPAM formed a mechanically robust ITUC composite hydrogel with integrated properties including temperature responsive volumetric change, photothermal responsiveness and electrical conductivity. The preparation process accredited a tremendous conductivity enhancement via the ice densification effect and low-temperature reaction of PAni was crucial for achieving resistive sensing of multimodal hydrogel

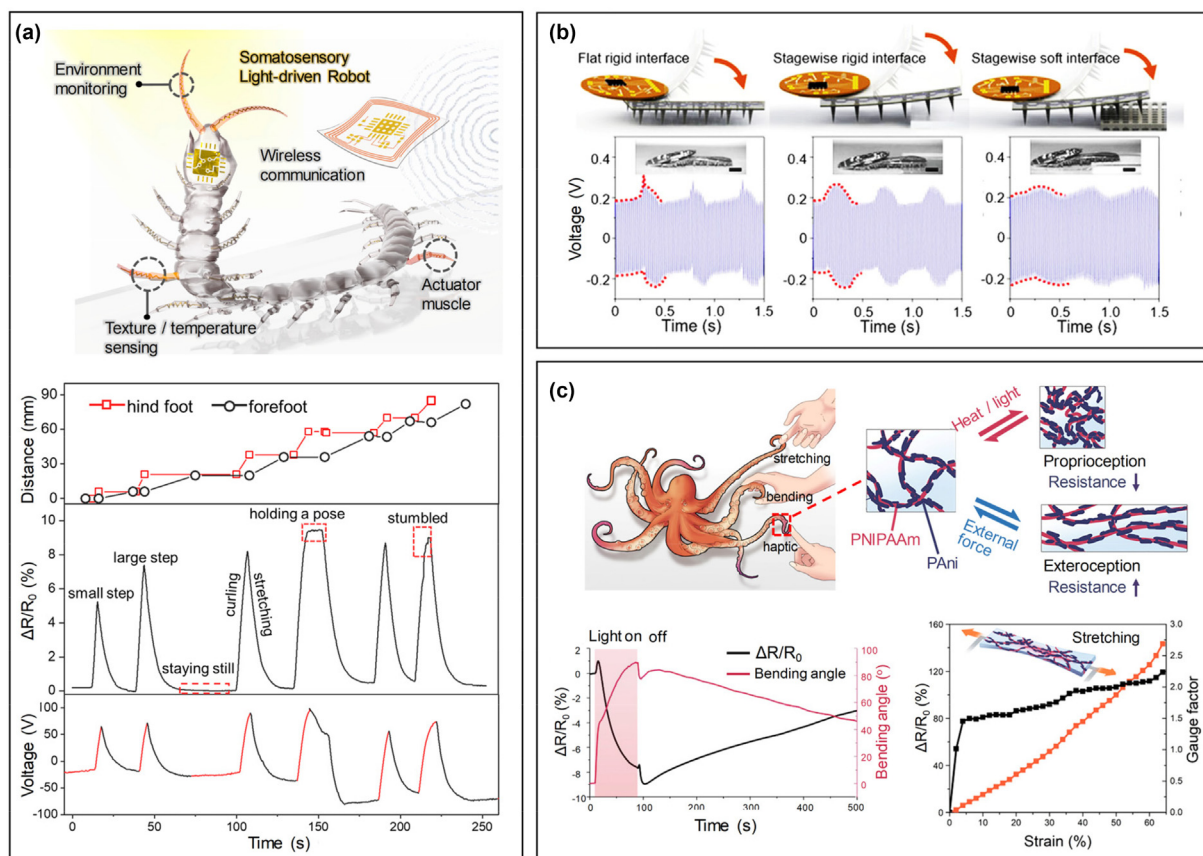


FIGURE 10

Soft robots with sensory functions. (a) Somatosensory, light-driven, thin-film robots with built-in, non-interfering piezoresistive strain sensor and pyroelectric temperature sensor [100]. (b) Magnetic soft millirobot with piezoelectric function that can detect different interfaces when actuated [273]. (c) Conductive and photothermal responsive hydrogel that is capable of multimodal sensory actuations [269].

deformations [269]. The monolithic hydrogel was capable of photothermal actuation and piezoresistive sensing, thereby executing robotic tasks including contraction, bending, object lifting, and object grasping while providing proprioceptive or exteroceptive feedback resistive change signals induced by photothermal actuation or external forces (Fig. 10c).

## Conclusions and perspective

Living organisms have complicated sensory and actuation systems, that feature great autonomy and define ways of interaction with the external world. A diversity of biological sensors and actuators ranging in complexity from the level of cells to that of animals, enable various functions and 'intelligent' behaviors. Hence, mimicking biological organisms offers the possibility to realize artificial intelligent robots across multiple length scales. Unlike conventional human-sized rigid robots, biology-inspired robots are made of downsized and compliant materials and structures, in which soft, active and responsive materials play a key role. The construction of a high-performance soft material machine requires not only active components, but also rational assembly/combination of materials and architectures, that possibly augment sensitivities, activate new functions, as well as create synergetic responses. This review specifically features progress in understanding complex and programmed locomotion in untethered soft systems and creation of locomotive

machines by the re-engineering of motility strategies seen in a variety of biological organisms. We delineate a roadmap toward the design of life-like locomotion driven by man-made material machines. We highlight design and construction principles that guide the engineering of soft materials and composites, and therefore enable fast reversible shape transformation of machines powered by energy sources in untethered ways. By mimicking the biological ways of body deformation and interaction with the surroundings, locomotive material machines under external controls are able to move forward on different terrains and swim in water, and show diverse biomimetic gaits, such as earthworm-like crawling, insect larvae-inspired jumping and sperm-like swimming. The biological out-of-equilibrium behaviors have inspired the exploration of imbalance actuations supported by different feedback mechanisms, enabling self-oscillation and autonomous movement of soft machines on the solid surface or in water. To further advance robotic locomotion to be more adaptive and purposeful, reconfigurable body deformation and multi-task operations performed by one soft machine are pursued.

The field of soft robotics strives to design fully artificial intelligent machines that are functional and autonomous. While materials have been developed, which in principle allow for integration of sensing and actuation in soft material machines, there remains a long way off before these machines could truly achieve

the biological level of intelligence and autonomy. As we push for practical use, further progress in soft machines should be judiciously designed with their end applications in mind, and the trade-offs between autonomy and functionality in different situations ought to be weighed out. As controlled by the man-made magnetic field generator, magnetic microrobots cannot deliver autonomous locomotion. However, magnetic microrobots have unique potential for applications inside a human body owing to high penetration depth of the magnetic field, and multimodal, reconfigurable locomotion produced by the exerted magnetic torques and forces. Autonomy of magnetic microrobots can be engineered by devising mechanisms combined with stimuli-responsive polymer material matrix, enabling adaptive tasks, such as spontaneous drug release in response to change of the physiological environment. Soft robots powered by available natural energy sources, such as light, heat and humidity, can have self-regulatory autonomous behaviors, and design of feedback loop mechanisms would create self-propelled locomotion under constant environmental conditions. Research on these environment responsive robots should involve the improvement and optimization of sensitivity, therefore creating autonomous robots that are able to be fueled by ambient energy sources, such as sunlight, low-grade heat or ambient humidity fluctuations. Progress of the soft material machines toward practical use demands material improvements, as well as advanced material and machine engineering technologies. For example, material properties, such as biocompatibility, biodegradation and strong magnetization, are sought for human-body use; high toughness and self-healing properties will improve robustness of the machine systems with the ability to withstand harsh and unpredictable environmental conditions. Advanced engineering technologies, such as printing, photolithography and kirigami/origami techniques, will ease the assembly, integration and shaping of multimaterials across all length scales, such as molecular and microstructure ordering, layout of multilayers, and 2D/3D geometrical shape patterning. Thereupon, collective endeavour and multipronged approaches will accelerate the development toward the next generation of advanced and practical robots with autonomy and intelligence.

### Declaration of Competing Interest

The authors declare that they have no known competing financial interests or personal relationships that could have appeared to influence the work reported in this paper.

### Acknowledgements

The research is supported by A\*STAR under its 2019 AME IRG & YIRG Grant Calls, A2083c0059 and the Advanced Research and Technology Innovation Centre (ARTIC), the National University of Singapore under Grant (project number: R261-518-014-720).

### References

- [1] G.-Z. Yang et al., *Sci. Robot.* 3 (14) (2018) eaar7650.
- [2] *Nat. Rev. Mater.* 3 (6) (2018) 71.
- [3] W. Hu et al., *Nature* 554 (7690) (2018) 81.
- [4] Y.C. Wu et al., *Sci. Robot.* 4 (32) (2019) eaax1594.
- [5] Y. Kim et al., *Sci. Robot.* 4 (33) (2019) eaax7329.
- [6] C. Walsh, *Nat. Rev. Mater.* 3 (6) (2018) 78.
- [7] H. Yuk et al., *Nat. Commun.* 8 (2017) 14230.
- [8] S.Y. Zhuo et al., *Sci. Adv.* 6 (5) (2020) eaax1464.
- [9] S. Terryn et al., *Sci. Robot.* 2 (9) (2020) eaan4268.
- [10] L. Hines et al., *Adv. Mater.* 29 (13) (2017) 1603483.
- [11] J.M. McCracken et al., *Adv. Mater.* 32 (20) (2020) 1906564.
- [12] S.I. Rich et al., *Nat. Electron.* 1 (2) (2018) 102.
- [13] H. Kim et al., *Mater. Today* 41 (2020) 243.
- [14] F. Lancia et al., *Nat. Rev. Chem.* 3 (9) (2019) 536.
- [15] M. Pilz da Cunha et al., *Chem. Soc. Rev.* 49 (18) (2020) 6568.
- [16] L. Hu et al., *Adv. Funct. Mater.* 30 (2) (2020) 1903471.
- [17] C. Bartolozzi et al., *Nat. Mater.* 15 (9) (2016) 921.
- [18] K. Xu et al., *Adv. Mater. Technol.* 4 (3) (2019) 1800628.
- [19] T.J. Wallin et al., *Nat. Rev. Mater.* 3 (6) (2018) 84.
- [20] K. Xu et al., *Adv. Funct. Mater.* 31 (39) (2021) 2007436.
- [21] K. Xu et al., *Adv. Mater.* 33 (18) (2021) 2008701.
- [22] Q. Zhang et al., *Adv. Funct. Mater.* 28 (1) (2018) 1703801.
- [23] T. Ding et al., *Nat. Commun.* 11 (1) (2020) 6006.
- [24] H. Zeng et al., *Adv. Mater.* 30 (24) (2018) 1870174.
- [25] D.D. Han et al., *Adv. Mater.* 28 (38) (2016) 8328.
- [26] Y. Hu et al., *Adv. Mater.* 28 (47) (2016) 10548.
- [27] B. Han et al., *Adv. Funct. Mater.* 28 (40) (2018) 1802235.
- [28] A. Miriyev et al., *Nat. Commun.* 8 (2017) 596.
- [29] M. Amjadi, M. Sitti, *ACS Nano* 10 (11) (2016) 10202.
- [30] S. Palagi, P. Fischer, *Nat. Rev. Mater.* 3 (6) (2018) 113.
- [31] M. Sitti, D.S. Wiersma, *Adv. Mater.* 32 (20) (2020) 1906766.
- [32] H. Zhou et al., *Chem. Rev.* 121 (8) (2021) 4999.
- [33] F. Ilievski et al., *Angew. Chem. Int. Ed.* 50 (8) (2011) 1890.
- [34] R.F. Shepherd et al., *Proc. Natl. Acad. Sci. U. S. A.* 108 (51) (2011) 20400.
- [35] R. Yoshida, T. Ueki, *NPG Asia Mater.* 6 (2014) e107.
- [36] P. Fratzl, F.G. Barth, *Nature* 462 (7272) (2009) 442.
- [37] H.C. Quan et al., *Nat. Rev. Mater.* 6 (3) (2021) 264.
- [38] M. Li et al., *Nat. Rev. Mater.* (2021), <https://doi.org/10.1038/s41578-021-00389-7>.
- [39] K. Kruse, F. Julicher, *Curr. Opin. Cell Biol.* 17 (1) (2005) 20.
- [40] K. Kinbara, T. Aida, *Chem. Rev.* 105 (4) (2005) 1377.
- [41] M.J. Liu et al., *Nature* 517 (7532) (2015) 68.
- [42] T.J. White, D.J. Broer, *Nat. Mater.* 14 (11) (2015) 1087.
- [43] T. Ikeda et al., *Angew. Chem., Int. Ed.* 46 (4) (2007) 506.
- [44] T. Ube, T. Ikeda, *Adv. Opt. Mater.* 7 (16) (2019) 1900380.
- [45] K. Urayama et al., *Phys. Rev. E* 71 (5) (2005) 051713.
- [46] Y.L. Yu et al., *Nature* 425 (6954) (2003) 145.
- [47] X. Pang et al., *Adv. Mater.* 31 (52) (2019) 1904224.
- [48] O.M. Wani et al., *Nat. Commun.* 8 (2017) 15546.
- [49] C. Ohm et al., *Adv. Mater.* 22 (31) (2010) 3366.
- [50] H.M.D. Bandara, S.C. Burdette, *Chem. Soc. Rev.* 41 (5) (2012) 1809.
- [51] M. Irie et al., *Chem. Rev.* 114 (24) (2014) 12174.
- [52] R. Klajn, *Chem. Soc. Rev.* 43 (1) (2014) 148.
- [53] M. Kondo et al., *Angew. Chem. Int. Ed.* 45 (9) (2006) 1378.
- [54] S.W. Ula et al., *Liq. Cryst. Rev.* 6 (1) (2018) 78.
- [55] L. Liu et al., *J. Am. Chem. Soc.* 139 (33) (2017) 11333.
- [56] A.H. Gelebart et al., *Adv. Mater.* 29 (18) (2017) 1606712.
- [57] L.Q. Yang et al., *Adv. Mater.* 20 (12) (2008) 2271.
- [58] H. Kim et al., *Adv. Funct. Mater.* 29 (48) (2019) 1905063.
- [59] Y.R. Sun et al., *Appl. Phys. Lett.* 100 (24) (2012) 241901.
- [60] S. Iamsaard et al., *Nat. Chem.* 6 (3) (2014) 229.
- [61] F. Lancia et al., *Nat. Commun.* 10 (2019) 4819.
- [62] J.J. Wie et al., *Nat. Commun.* 7 (1) (2016) 13260.
- [63] L.T. de Haan et al., *Angew. Chem., Int. Ed.* 51 (50) (2012) 12469.
- [64] S.J. Asshoff et al., *Angew. Chem., Int. Ed.* 56 (12) (2017) 3261.
- [65] R. Yang, Y. Zhao, *Angew. Chem., Int. Ed.* 56 (45) (2017) 14202.
- [66] B. Zuo et al., *Nat. Commun.* 10 (4539) (2019) 4539.
- [67] Y.B. Zhang et al., *Sci. Adv.* 6 (9) (2020) eaay8606.
- [68] S.J. Kim et al., *Adv. Mater.* 30 (12) (2018) 1706547.
- [69] S. Timoshenko, *J. Opt. Soc. Am.* 11 (3) (1925) 233.
- [70] C.L. van Oosten et al., *Nat. Mater.* 8 (8) (2009) 677.
- [71] Y.Y. Xiao et al., *Adv. Mater.* 31 (36) (2019) 1903452.
- [72] Y.L. Tai et al., *Adv. Mater.* 28 (23) (2016) 4665.
- [73] B.E. Trembl et al., *Adv. Mater.* 30 (7) (2018) 1705616.
- [74] D.D. Han et al., *Adv. Mater.* 27 (2) (2015) 332.
- [75] G.F. Cai et al., *Sci. Adv.* 5 (7) (2019) eaaw7956.
- [76] J. Gong et al., *Adv. Mater.* 29 (16) (2017) 1605103.
- [77] Y. Hu et al., *ACS Nano* 15 (3) (2021) 5294.
- [78] L. Yang et al., *Adv. Funct. Mater.* 31 (27) (2021) 2101378.

- [79] J. Troyano et al., *Adv. Mater.* 31 (21) (2019) 1808235.
- [80] X.B. Zhang et al., *Nano Lett.* 11 (8) (2011) 3239.
- [81] W.A. Xu et al., *Sci. Adv.* 3 (10) (2017) e1701084.
- [82] Y. Cheng et al., *ACS Nano* 13 (11) (2019) 13176.
- [83] C.X. Ma et al., *Adv. Funct. Mater.* 28 (7) (2018) 1704568.
- [84] Q. Zhao et al., *Nat. Commun.* 5 (2014) 4293.
- [85] W.X. Fan et al., *Sci. Adv.* 5 (4) (2019) eaav7174.
- [86] R.C. Luo et al., *Adv. Funct. Mater.* 25 (47) (2015) 7272.
- [87] X. Pan et al., *Adv. Funct. Mater.* 31 (18) (2021) 2100465.
- [88] X.S. Qian et al., *Nat. Nanotechnol.* 14 (11) (2019) 1048.
- [89] Y. He et al., *Adv. Funct. Mater.* 31 (26) (2021) 2101291.
- [90] L.P. Li et al., *ACS Appl. Mater. Interfaces* 10 (17) (2018) 15122.
- [91] L.D. Zhang et al., *Adv. Mater.* 29 (37) (2017) 1702231.
- [92] T. van Manen et al., *Mater. Today* 21 (2) (2018) 144.
- [93] J. Deng et al., *J. Am. Chem. Soc.* 138 (1) (2016) 225.
- [94] L. Liu et al., *Adv. Funct. Mater.* 26 (7) (2016) 1021.
- [95] M. Kanik et al., *Science* 365 (6449) (2019) 145.
- [96] J. Kim et al., *Science* 335 (6073) (2012) 1201.
- [97] E. Palleau et al., *Nat. Commun.* 4 (2013) 2257.
- [98] X. Peng et al., *Adv. Funct. Mater.* 26 (25) (2016) 4491.
- [99] B. Han et al., *Adv. Mater.* 31 (5) (2019) 1806386.
- [100] X.Q. Wang et al., *Adv. Mater.* 32 (21) (2020) 2000351.
- [101] Q.H. Liu et al., *Nat. Commun.* 9 (2018) 846.
- [102] D. Wirthl et al., *Sci. Adv.* 3 (6) (2017) e1700053.
- [103] C.J. Wang et al., *Adv. Mater.* 30 (13) (2018) 1706695.
- [104] L.Z. Chen et al., *Adv. Funct. Mater.* 29 (5) (2019) 1806057.
- [105] X.-Q. Wang et al., *Nat. Commun.* 9 (1) (2018) 3438.
- [106] L.L. Yang et al., *Adv. Funct. Mater.* 30 (15) (2020) 1908842.
- [107] L. Hu et al., *ACS Nano* 9 (5) (2015) 4835.
- [108] X. Liu et al., *Mater. Today* 36 (2020) 102.
- [109] L. Ionov, *Mater. Today* 17 (10) (2014) 494.
- [110] X. Le et al., *Adv. Sci.* 6 (5) (2019) 1801584.
- [111] K. Sano et al., *Angew. Chem., Int. Ed.* 57 (10) (2018) 2532.
- [112] S.M. Zhang et al., *Nat. Mater.* 9 (7) (2010) 594.
- [113] M.T.I. Mredha et al., *Adv. Mater.* 30 (9) (2018) 1704937.
- [114] A.S. Gladman et al., *Nat. Mater.* 15 (4) (2016) 413.
- [115] J. Ramon-Azcon et al., *Adv. Mater.* 25 (29) (2013) 4028.
- [116] L.L. Wu et al., *ACS Nano* 8 (5) (2014) 4640.
- [117] K. Sano et al., *Angew. Chem., Int. Ed.* 57 (38) (2018) 12508.
- [118] P. Xue et al., *Angew. Chem. Int. Ed.* 60 (7) (2021) 3390.
- [119] H.F. Zhang et al., *Nat. Mater.* 4 (10) (2005) 787.
- [120] H. Bai et al., *Chem. Mater.* 25 (22) (2013) 4551.
- [121] J.J. Wu et al., *J. Mater. Chem.* 22 (34) (2012) 17449.
- [122] Y.S. Kim et al., *Nat. Mater.* 14 (10) (2015) 1002.
- [123] M.C. Zhang et al., *Adv. Sci.* 7 (6) (2020) 1903048.
- [124] R.M. Erb et al., *Nat. Commun.* 4 (2013) 1712.
- [125] Y.Q. Jiang et al., *Nat. Commun.* 10 (2019) 4111.
- [126] C.Q. Zhao et al., *Nature* 580 (7802) (2020) 210.
- [127] C. Yang, Z. Suo, *Nat. Rev. Mater.* 3 (6) (2018) 125.
- [128] M. Zrinyi et al., *Polym. Gels Networks* 5 (5) (1997) 415.
- [129] M. Zrinyi et al., *J. Chem. Phys.* 104 (21) (1996) 8750.
- [130] M. Li et al., *Proc. Natl. Acad. Sci. U. S. A.* 115 (32) (2018) 8119.
- [131] D. Collin et al., *Macromol. Rapid Commun.* 24 (12) (2003) 737.
- [132] S. Fusco et al., *ACS Appl. Mater. Interfaces* 7 (12) (2015) 6803.
- [133] E. Diller, M. Sitti, *Adv. Funct. Mater.* 24 (28) (2014) 4397.
- [134] M. Khoo, C. Liu, *Sens. Actuators, A* 89 (3) (2001) 259.
- [135] S.Y. Chin et al., *Sci. Robot.* 2 (2) (2017) eaah6451.
- [136] V. Magdanz et al., *Adv. Mater.* 28 (21) (2016) 4084.
- [137] X.H. Zhao et al., *Proc. Natl. Acad. Sci. U. S. A.* 108 (1) (2011) 67.
- [138] J. Kim et al., *Nat. Mater.* 10 (10) (2011) 747.
- [139] H. Lee et al., *Nat. Mater.* 9 (9) (2010) 745.
- [140] E. Diller et al., *Appl. Phys. Lett.* 104 (17) (2014) 174101.
- [141] R. Dreyfus et al., *Nature* 437 (7060) (2005) 862.
- [142] Y. Kim et al., *Nature* 558 (7709) (2018) 274.
- [143] J.Z. Cui et al., *Nature* 575 (7781) (2019) 164.
- [144] J.K. Mu et al., *Sci. Adv.* 1 (10) (2015) e1500533.
- [145] L.L. Zhu et al., *Soft Matter* 13 (25) (2017) 4441.
- [146] L. Mahadevan et al., *Proc. Natl. Acad. Sci. U. S. A.* 101 (1) (2004) 23.
- [147] R.R. Kohlmeier, J. Chen, *Angew. Chem., Int. Ed.* 52 (35) (2013) 9234.
- [148] M. Ji et al., *Adv. Funct. Mater.* 24 (34) (2014) 5412.
- [149] X.L. Lu et al., *Adv. Mater.* 30 (14) (2018) 1706597.
- [150] H. Zeng et al., *Adv. Mater.* 27 (26) (2015) 3883.
- [151] L.Z. Chen et al., *ACS Nano* 9 (12) (2015) 12189.
- [152] B. Shin et al., *Sci. Robot.* 3 (14) (2018) eaar2629.
- [153] X. Wang et al., *Mater. Today* 35 (2020) 42.
- [154] W. Wang et al., *Bioinspir. Biomim.* 9 (4) (2014) 046006.
- [155] C. Li et al., *Sci. Robot.* 5 (49) (2020) eabb9822.
- [156] L.I. van Griethuysen, B.A. Trimmer, *Biol. Rev. Cambridge Philos. Soc.* 89 (3) (2014) 656.
- [157] M. Rogoz et al., *Adv. Opt. Mater.* 4 (11) (2016) 1689.
- [158] H. Zeng et al., *Macromol. Rapid Commun.* 39 (1) (2018) 1700224.
- [159] H.J. Lu et al., *Nat. Commun.* 9 (2018) 3944.
- [160] H.R. Gu et al., *Nat. Commun.* 11 (1) (2020) 2637.
- [161] M. Wang et al., *Chem. Commun.* 56 (55) (2020) 7597.
- [162] M. Rogoz et al., *Macromol. Rapid Commun.* 40 (16) (2019) 1900279.
- [163] N. Saga, T. Nakamura, *Smart Mater. Struct.* 13 (3) (2004) 566.
- [164] H. Marvi et al., *J. R. Soc. Interface* 10 (84) (2013) 20130188.
- [165] Z.F. Sun et al., *Angew. Chem., Int. Ed.* 57 (48) (2018) 15772.
- [166] X. Liu et al., *J. Mater. Chem. B* 4 (45) (2016) 7293.
- [167] A.H. Gelebart et al., *Nature* 546 (7660) (2017) 632.
- [168] R.H. Armour, J.F.V. Vincent, *J. Bionic Eng.* 3 (4) (2006) 195.
- [169] X. Zhang et al., *Nat. Commun.* 5 (2014) 2983.
- [170] Y. Sugiyama, S. Hirai, *Int. J. Robot. Res.* 25 (5–6) (2006) 603.
- [171] X. Lu et al., *Adv. Mater.* 29 (28) (2017) 1606467.
- [172] Y. Zhang et al., *J. Mater. Chem. A* 5 (28) (2017) 14604.
- [173] T. Taniguchi et al., *Nat. Commun.* 9 (2018) 538.
- [174] S. Wang et al., *Nat. Commun.* 11 (1) (2020) 4359.
- [175] Y.C. Cheng et al., *Adv. Mater.* 32 (7) (2020) 1906233.
- [176] Y. Cheng et al., *Adv. Funct. Mater.* 31 (32) (2021) 2101825.
- [177] H.T. Lin et al., *Bioinspir. Biomim.* 6 (2) (2011) 026007.
- [178] J. Brackenburg, *Nature* 390 (6659) (1997) 453.
- [179] C. Zhang et al., *Robot. Auton. Syst.* 124 (2020) 103362.
- [180] L.Q. Shui et al., *Soft Matter* 13 (44) (2017) 8223.
- [181] O. Bolmin et al., *J. Exp. Biol.* 222 (12) (2019) jeb196683.
- [182] M.A. Ashley-Ross et al., *Zoology* 117 (1) (2014) 7.
- [183] G.M. Farley et al., *J. Exp. Biol.* 222 (15) (2019) jeb201v129.
- [184] H. Li, J. Wang, *ACS Appl. Mater. Interfaces* 11 (10) (2019) 10218.
- [185] H. Arazoe et al., *Nat. Mater.* 15 (10) (2016) 1084.
- [186] Y. Hu et al., *Adv. Funct. Mater.* 27 (44) (2017) 1704388.
- [187] C.Y. Ahn et al., *Adv. Mater. Technol.* 4 (7) (2019) 1900185.
- [188] M.K. Panda et al., *Nat. Commun.* 5 (2014) 4811.
- [189] R. Medishetty et al., *Chem. Mater.* 27 (5) (2015) 1821.
- [190] G. Gao et al., *ACS Appl. Mater. Interfaces* 10 (48) (2018) 41724.
- [191] J. Jeon et al., *Mater. Today* 49 (2021) 97.
- [192] M. Li et al., *Nat. Commun.* 11 (1) (2020) 3988.
- [193] B.U. Felderhof, R.B. Jones, *Physica A* 202 (1–2) (1994) 119.
- [194] E.M. Purcell, *Am. J. Phys.* 45 (1) (1977) 3.
- [195] M. Salta et al., *Phil. Trans. R. Soc. A* 368 (1929) (2010) 4729.
- [196] K.F. Jarrell, M.J. McBride, *Nat. Rev. Microbiol.* 6 (6) (2008) 466.
- [197] H.C. Berg, *Annu. Rev. Biochem.* 72 (2003) 19.
- [198] C.J. Brokaw, *J. Cell Biol.* 114 (6) (1991) 1201.
- [199] E.W. Knight-Jones, *J. Cell Sci.* s3-95 (32) (1954) 503.
- [200] K.E. Peyer et al., *Chem. Eur. J.* 19 (1) (2013) 28.
- [201] S. Tottori et al., *Adv. Mater.* 24 (6) (2012) 811.
- [202] A.M. Maier et al., *Nano Lett.* 16 (2) (2016) 906.
- [203] H.W. Huang et al., *Sci. Adv.* 5 (1) (2019) eaau1532.
- [204] D. Walker et al., *Nano Lett.* 15 (7) (2015) 4412.
- [205] A. Mourran et al., *Adv. Mater.* 29 (2) (2017) 1604825.
- [206] H.W. Huang et al., *Nat. Commun.* 7 (2016) 12263.
- [207] V. Magdanz et al., *Adv. Mater.* 29 (24) (2017) 1606301.
- [208] I.S.M. Khalil et al., *Appl. Phys. Lett.* 109 (3) (2016) 033701.
- [209] M. Roper et al., *Proc. R. Soc. A* 464 (2092) (2008) 877.
- [210] S. Palagi et al., *Nat. Mater.* 15 (6) (2016) 647.
- [211] W.S. Chu et al., *Int. J. Precis. Eng. Manuf.* 13 (7) (2012) 1281.
- [212] J.C. Nawroth et al., *Nat. Biotechnol.* 30 (8) (2012) 792.
- [213] B. Bhandari et al., *Int. J. Precis. Eng. Manuf.* 13 (1) (2012) 141.
- [214] P.S. Xiao et al., *Adv. Sci.* 3 (6) (2016) 1500438.
- [215] I.A. Anderson et al., *J. Appl. Phys.* 112 (4) (2012) 041101.
- [216] T.F. Li et al., *Sci. Adv.* 3 (4) (2017) e1602045.
- [217] Z. Ren et al., *Nat. Commun.* 10 (1) (2019) 2703.
- [218] M. Camacho-Lopez et al., *Nat. Mater.* 3 (5) (2004) 307.
- [219] G.H. Kwon et al., *Small* 4 (12) (2008) 2148.
- [220] H. Shahsavani et al., *Proc. Natl. Acad. Sci. U. S. A.* 117 (10) (2020) 5125.
- [221] S. Maeda et al., *Adv. Mater.* 19 (21) (2007) 3480.
- [222] X.M. He et al., *Nature* 487 (7406) (2012) 214.
- [223] T.J. White et al., *Soft Matter* 4 (9) (2008) 1796.

- [224] M.M. Ma et al., *Science* 339 (6116) (2013) 186.
- [225] S. Serak et al., *Soft Matter* 6 (4) (2010) 779.
- [226] K.M. Lee et al., *Adv. Funct. Mater.* 21 (15) (2011) 2913.
- [227] K. Kumar et al., *Nat. Commun.* 7 (2016) 11975.
- [228] H. Zeng et al., *Nat. Commun.* 10 (2019) 5057.
- [229] R. Tang et al., *ACS Appl. Mater. Interfaces* 7 (16) (2015) 8393.
- [230] F.J. Ge et al., *Angew. Chem., Int. Ed.* 57 (36) (2018) 11758.
- [231] R. Lan et al., *Adv. Mater.* 32 (14) (2020) 1906319.
- [232] J. Sun et al., *Adv. Funct. Mater.* 31 (33) (2021) 2103311.
- [233] L. Yu, H.F. Yu, *ACS Appl. Mater. Interfaces* 7 (6) (2015) 3834.
- [234] X. Dong et al., *ACS Appl. Mater. Interfaces* 12 (5) (2020) 6460.
- [235] Y. Zhao et al., *Sci. Robot.* 4 (33) (2019) eaax7112.
- [236] Z. Hu et al., *Nat. Commun.* 12 (1) (2021) 3211.
- [237] L. Zhang et al., *Nat. Commun.* 6 (1) (2015) 7429.
- [238] Z. Zhao et al., *Proc. Natl. Acad. Sci. U. S. A.* 117 (16) (2020) 8711.
- [239] Y. Wang et al., *Matter* 1 (3) (2019) 626.
- [240] E. Uchida et al., *Nat. Commun.* 6 (1) (2015) 7310.
- [241] X. Chen et al., *Nat. Commun.* 6 (1) (2015) 7346.
- [242] A. Baumann et al., *Nat. Mater.* 17 (6) (2018) 523.
- [243] C. Ahn et al., *ACS Appl. Mater. Interfaces* 10 (30) (2018) 25689.
- [244] A. Kotikian et al., *Sci. Robot.* 4 (33) (2019) eaax7044.
- [245] S. Ma et al., *Angew. Chem. Int. Ed.* 58 (9) (2019) 2655.
- [246] F. Zhai et al., *Matter* 4 (10) (2021) 3313.
- [247] Z. Li et al., *Sci. Robot.* 6 (61) (2021) eabi4523.
- [248] D. Martella et al., *Adv. Mater.* 29 (42) (2017) 1704047.
- [249] M. Cianchetti et al., *Nat. Rev. Mater.* 3 (6) (2018) 143.
- [250] A. Billard, D. Kragic, *Science* 364 (6446) (2019) eaat8414.
- [251] S. Fusco et al., *Adv. Mater.* 26 (6) (2014) 952.
- [252] J. Li et al., *Sci. Robot.* 2 (4) (2017) eaam6431.
- [253] S.A. Morin et al., *Science* 337 (6096) (2012) 828.
- [254] X. Du et al., *Adv. Funct. Mater.* 30 (10) (2020) 1909202.
- [255] X.-Q. Wang et al., *Adv. Opt. Mater.* 2 (7) (2014) 652.
- [256] C. Larson et al., *Science* 351 (6277) (2016) 1071.
- [257] Y.-C. Lai et al., *Adv. Mater.* 30 (28) (2018) 1801114.
- [258] Z. Ren et al., *Sci. Adv.* 7 (27) (2021) eabh2022.
- [259] A. Cangialosi et al., *Science* 357 (6356) (2017) 1126.
- [260] N.W. Bartlett et al., *Science* 349 (6244) (2015) 161.
- [261] T. Li et al., *Sci. Adv.* 7 (2) (2021) eabe3184.
- [262] F.G. Downs et al., *Nat. Chem.* 12 (4) (2020) 363.
- [263] X. Kuang et al., *Adv. Mater.* 33 (30) (2021) 2102113.
- [264] J. Lou et al., *Adv. Funct. Mater.* 31 (11) (2021) 2008328.
- [265] Z. Hu et al., *Nat. Commun.* 11 (1) (2020) 5780.
- [266] K. He et al., *Adv. Mater.* 32 (4) (2020) 1905399.
- [267] R.L. Truby et al., *Adv. Mater.* 30 (15) (2018) 1706383.
- [268] I.M.V. Meerbeek et al., *Sci. Robot.* 3 (24) (2018) eaau2489.
- [269] Y. Zhao et al., *Sci. Robot.* 6 (53) (2021) eabd5483.
- [270] H. Yang et al., *Sci. Robot.* 4 (33) (2019) eaax7020.
- [271] A. Kotikian et al., *Adv. Mater.* 33 (27) (2021) 2101814.
- [272] C.-Y. Lo et al., *Mater. Today* 50 (2021) 35.
- [273] H. Lu et al., *Adv. Sci.* 7 (13) (2020) 2000069.